An individual fly-handling robot allows high throughput longitudinal measurement of *Drosophila* social networks.

university of groningen / faculty of behavioural and social sciences

T. Alisch

(s2348853)

Juli 2017

Major Thesis MSc Programme Behavioural and Cognitive Neurosciences

Faculty of Mathematics and Natural Sciences

University of Groningen

Day-to-day supervisor: B. L. de Bivort

Evaluator: J.-C. Billeter

An individual fly-handling robot allows high throughput longitudinal measurement of Drosophila social networks.

Drosophila melanogaster exhibits quantifiable non-random patterns during social interactions that can be summarized in a social interaction network (SIN). Parameters describing SINs, such as frequency and length of interactions, have been proposed to be under the influence of genetic variation and shown to remain stable within experimental trials (Schneider, Dickinson, & Levine, 2012). However, it is not yet established whether and to what extent SIN parameters on the group and individual level change over longer periods of time. Longitudinal SIN measurements are arduous and error-prone to perform by hand. For example, manually handling individual flies across time cumulatively increases chances for human error. To remedy this, we developed an individual fly-handling robot capable of autonomously performing high throughput longitudinal experiments. Here, we demonstrate that the robot 1) autonomously collects newly eclosed flies, 2) sets up multiple longitudinal closed-circuit SIN analyses with dozens of fruit flies, and 3) reliably maintains individual flies' identity across experiments. Using the robot to autonomously run a novel social behavior assay, we found that 1) *Drosophila melanogaster* exhibit persistent idiosyncrasies in affiliative behavior, 2) affiliative behavior is diminished with impaired visual or olfactory inputs, 3) persistence in affiliative behavior requires olfactory and visual inputs, and 4) SIN structure is topologically stable over time. Potential of the robot for the use in other paradigms is discussed.

In recent years, automated experimental setups have been increasingly employed in a variety of scientific fields. Particularly in biology and the neurosciences, automated methods have proven to be irreplaceable in allowing researchers involve large numbers of model organisms without sacrificing efficiency and precision. The term 'automation' comprises a variety of fundamentally different systems that, for example, allow large-scale movement-tracking and even analyses of behavior (Branson, Robie, Bender, Perona, & Dickinson, 2009), allow investigation of behaviors that would otherwise be difficult to elicit in a controlled manner in the laboratory (Card & Dickinson, 2008), facilitate 24/7 observation of individuals (Pfeiffenberger, Lear, Keegan, & Allada, 2010), or automate pre-experimental phenotyping and selection, reducing manual handling time requirements (Medici, Vonesch, Fry, & Hafen, 2015). Automation is increasingly advantageous over conventional manual methods as experimental duration expands. Besides convenience and budgetary reasons, automated platforms have the potential to ensure equal and unbiased treatment of individuals, reduce the potential for human error, and allow 24/7 experimentation by managing handling of individual animals.

Automated handling and observation platforms have already been successfully developed for larval zebrafish, *Caenorhabditis elegans* (Albrecht & Bargmann, 2011; Chalasani et al., 2007; Chung et al., 2011; Crane et al., 2012) and recently *Drosophila melanogaster* (Kumar, Sun, Zou, & Hong, 2016; Savall, Ho, Huang, Maxey, & Schnitzer, 2015). Commonly, platforms have been designed to automate very sophisticated specific sequences under precise conditions. For example, a robotic arm might pick single fruit flies before imaging and categorizing body dimension parameters to ultimately perform neurosurgery, but might rely on operation in complete darkness. Should the necessity to alter stimulus conditions inadvertently arise, existing automated systems may not perform at full capacity. In a similar vein, existing highly specialized robots may likely not be usable in future paradigms for which they were not originally designed. Adopting a modular approach in which entire experimental assays can be switched out ad libitum while the general robot architecture remains stationary would prevent the platform from being rendered obsolete. Additionally, existing automated robotic systems require both

manual animal supply as well as manual post-experimental clean-up. Besides saving time, automating these processes would maximize treatment homogeneity and rearing equality as human handling is minimized at every step of experimentation. To meet these demands, we created an individual fly-handling modular robot capable of unsupervised virgining and subsequent closed-circuit 24/7 high-throughput experimentation with few environmental constrains.

Affiliative behavior and social interaction networks

To demonstrate the robot's capabilities, we decided to investigate persistence and idiosyncrasy in affiliative behavior in *Drosophila melanogaster*. Individual-to-individual differences in humans and animals describe the well-documented phenomenon of persistent idiosyncrasies in observed behavior in otherwise homogenous conditions (Buchanan, Kain, & de Bivort, 2015; Kain, Stokes, & de Bivort, 2012; Kain et al., 2015). For example, population level variance in a quantifiable behavior might be caused by individuals persistently behaving with little within-individual variance themselves. In animals, individual differences arise even in inbred, isogenic individuals and remain stable in their magnitude and direction across each individual's lifetime (Buchanan et al., 2015). Interestingly, observed differences and biases in behavior are not heritable but appear to at least partially be modulated by differences in morphology of neurons implied to the processing of sensory information related to the behavior. For example, silencing columnar neurons in the central complex, involved in motor planning and execution, increases population-level biases in locomotor handedness, flies' overall tendency to turn left- or rightwards, by shifting individuals' behavior towards the extremes (Buchanan et al., 2015). Indeed, the notion that individual differences are not directly genetically determined may be beneficial to the fitness of the population in that a given behavior has the potential to remain variable in the face of narrow sexual selection (Dall, Houston, & McNamara, 2004), increasing fitness in face of transient selective pressure (Kain et al., 2015). This may especially be true when more than one extreme in the variability of the behavior in question is relevant for survival. For example, direction of phototaxis in *Drosophila*

melanogaster, i.e., the tendency to walk towards or away from a light source, may either be rewarding or punishing for the individual, depending on the environmental context.

Still, when observed outside of isolation, an individual's behavior is not under control of the individual alone but influenced by the behaviors of other group members. For example, even in invertebrates, such as the fruit fly *Drosophila melanogaster*, informed individuals may actively communicate useful information with uninformed individuals in the same social network, thus affecting their behavior (Alem et al., 2016; Kacsoh, Bozler, Ramaswami, & Bosco, 2015; Pasquaretta et al., 2016; Ramdya et al., 2014). In a given social network, the mode and effectiveness of communication is influenced by individuals' personality, a tendency for behavior to be biased towards a certain direction with a certain magnitude (Pike, Samanta, Lindstrom, & Royle, 2008). Specifically, personality here refers to individual differences in tendencies to approach or avoid, for example, predatory stimuli (Kacsoh et al., 2015)

Social networks are commonly used to qualitatively and quantitatively describe interactions between individuals within a group. Further, measures of tangible behaviors can be used to determine descriptions of abstract relationships between individuals. Network structure can be characterized by 1) its size, i.e., the amount of individuals composing the network; 2) the amount of total information flow, i.e., the absolute strength and amount of all connections between individuals; and 3) its dimension (or treewidth), i.e., homo- or heterogeneity in the amount of connections between individuals leading to more uniform (e.g., circular) or more heteromorphic network shapes. In general, social network structure depends on sent and received information across individuals. Individuals, or 'nodes' in a network, can be characterized by 1) their relative position within the network (medial or lateral); 2) the amount and strength of connections with other nodes; and 3) the amount of information flowing through the node, i.e., the nodes' importance as an information relay. Using descriptions of network structure and individual nodes, more sophisticated network analyses may be performed. However, not all sensory information modes (e.g., visual and tactile) necessarily affect network interactions equally. For example, even though

visual and auditory *Drosophila* mutants exhibit normal social network structure despite comparatively lower flow of information, olfactory mutants showed considerable deterioration of network parameters (Schneider et al., 2012). In social animals, the olfactory system generally appears to play an important role in forming social networks. This is evident, for example, both in the magnitude of relationship disruption sufferers of anosmia report (Croy, Bojanowski, & Hummel, 2013), as well as increased anxiety-like responses observed in anosmic zebrafish (Abreu, Giacomini, Kalueff, & Barcellos, 2016). Notably, in a given human or animal population, complete loss of olfaction occurs rather rarely compared to individual-to-individual morphological and functional variations in the olfactory system. In fact, even highly inbred isogenic strains of *Drosophila* exhibit substantial variability in the degree and direction of their preference for certain odors (Honegger, Smith, Turner, & de Bivort, 2016). While it appears evident that individuals' diminished sensory information flow disrupts network structure on the group level, effects on affiliative behavior of individuals and a distinct time course of disruption have not yet been established. At least in humans, social network parameters have been found to remain stable even over long periods of time (up to 9 months), whereas individual characteristics within the network appear more volatile (Kossinets, 2006). Similarly, stability in *Drosophila* social network structure could be established at least within short (30 minutes) experimental trial duration (Pasquaretta et al., 2016).

Novel social interaction network paradigm

Due to technical limitations, questions about longer-term persistence in affiliative behavior on the individual level, as well as in social interaction network (SIN) structure on the group level so far have eluded answering (Pasquaretta et al., 2016; Schneider et al., 2012). Still, within single experimental sessions, there indeed appears to be distinct persistence in SIN parameters, such as degree of the network. The same technical difficulties constraining investigation of persistence also prohibit examination of idiosyncrasies in affiliative behavior. To extend investigation to multiple time points and the individual level, several practical challenges have to be overcome. First, individual fly' identity has to be reliably maintained, preferably without perceivable visual markers, such as tags or colored markings, so as not to

confound affiliative behavior. Second, flies have to be moved between experimental and housing areas to allow feeding and maintain health. Third, signal capture has to be simplified to allow for longer observation times and high-throughput measurements. Conventionally, fly identity and movement are analyzed using sophisticated softwares exhibiting very high accuracy (Colomb, Reiter, Blaszkiewicz, Wessnitzer, & Brembs, 2012; Gibson et al., 2015). However unlikely errors are, due to considerable carry-over effect of wrongful identification of even single flies, experiments have to be limited in scope. Specifically, if the identity of two flies is swapped on even a single frame, subsequent frames retain wrongful identity, effectively contaminating future data. Either network size, number of repetitions, and duration of observation need be limited to minimize error potential. In effect, this restricts conventional paradigms to only short sessions of under an hour and groups of around 10 individuals. In summary, due to technical limitations of traditional paradigms, longitudinal, repeat observations, as well as large sample sizes are challenging.

We propose a novel paradigm to solve this issue. SIN investigations in *Drosophila* traditionally focus on observing real-time interactions between individuals in spatially and temporally constricted context (Kaur, Simon, Chauhan, & Chauhan, 2015; Pasquaretta et al., 2016; Schneider et al., 2012; Simon et al., 2012). In other words, to recreate a natural setting, groups of flies are observed together in an arena at the same time. In contrast, most social network analyses in humans are performed on abstract measures of affiliative behavior, for example, the amount of content of electronic messages between individuals, effectively removing spatial or temporal constrains (Kossinets, 2006). While sacrificing ecological richness, adopting a similar approach in *Drosophila* resolves most issues with existing paradigms. Parallelly analyzing pairwise measures of affiliative behavior between dyads of isolated individual group members 1) allows high-throughput processing, 2) allows use of faster movement tracking software, in turn permitting longer observations, and 3) simplifies retaining individuals' identity. Additionally, measures of interactions between individuals are less confounded by spatiotemporal constrains or competing behaviors, such as exploration. That is, measures of dyad affiliative behavior can be captured at every time point and are informative regardless of context.

In conclusion, we created an individual fly-handling robot capable of unsupervised virgining and closed-circuit high-throughput experimentation. Here, we demonstrate the robot's potential in a novel paradigm for the investigation of persistence and idiosyncrasy in affiliative behavior, as well as social interaction networks. Using the robot to autonomously run longitudinal social assays, we found that 1) *Drosophila melanogaster* exhibit persistent idiosyncrasies in affiliative behavior, 2) affiliative behavior is diminished with impaired visual or olfactory inputs, 3) affiliative behavior persistence requires olfactory and visual inputs, and 4) social interaction network structure is topologically stable over time.

Results

Affiliative behavior

All results presented here were obtained using a novel high-throughput affiliative behavior assay for *Drosophila melanogaster*. We placed 2 flies (referred to as a dyad) in a circular arena evenly divided by a wall, referred to as the fence. Different types of fences were used (e.g., solid clear, perforated clear, or perforated black) to separate dyad flies. **Figure 1** shows outlines and dimensions of a high-throughput tray containing 96 arenas fitting 182 flies. We assess dyad affiliative behavior by analyzing flies' movement and assessing in how far flies' position is influenced by dyad neighbor position.

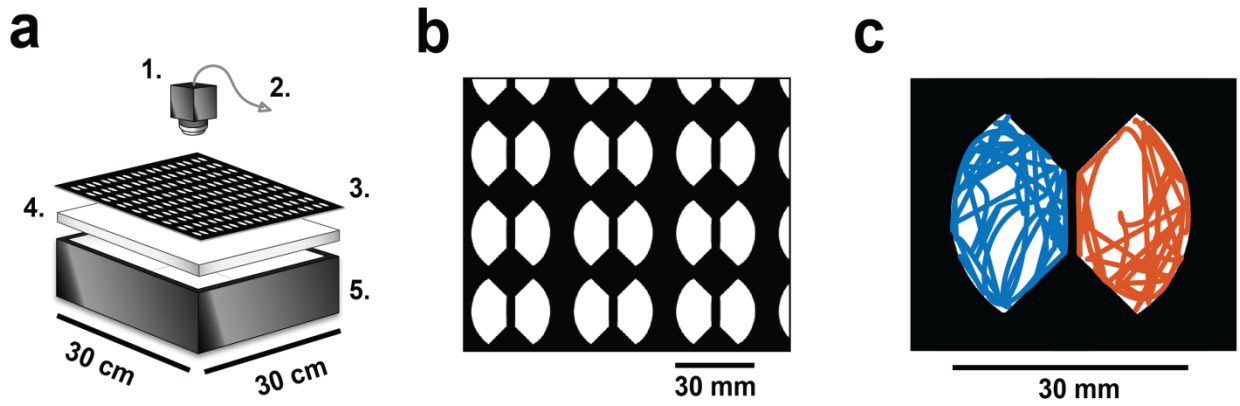

Figure 1. Experimental setup using affiliative behavior module. **a**: Behavioral module dimensions and setup in observation box. *1.*Digital camera; *2.* Connection to computer; *3.* 81-arena tray; *4.* Acrylic diffuser; *5.* LED-IR-illumination bottom. **b**: Top-view of a tray segment and single arena dimension. **c**: Single arena with example paths of two flies over 2 minutes.

First, we establish that 1) different types of fences used to separate flies within dyads either allow or restrict flow of different sensory information and 2) sensory information flow within dyads is

necessary for flies in dyads to modulate their social distance. We posit that the degree of social distance modulation is captured by the absolute correlation between flies' distances to the fence across the experiment. We refer to the correlation between two flies' distances to the fence as 'interaction index' (**Fig. 2**).

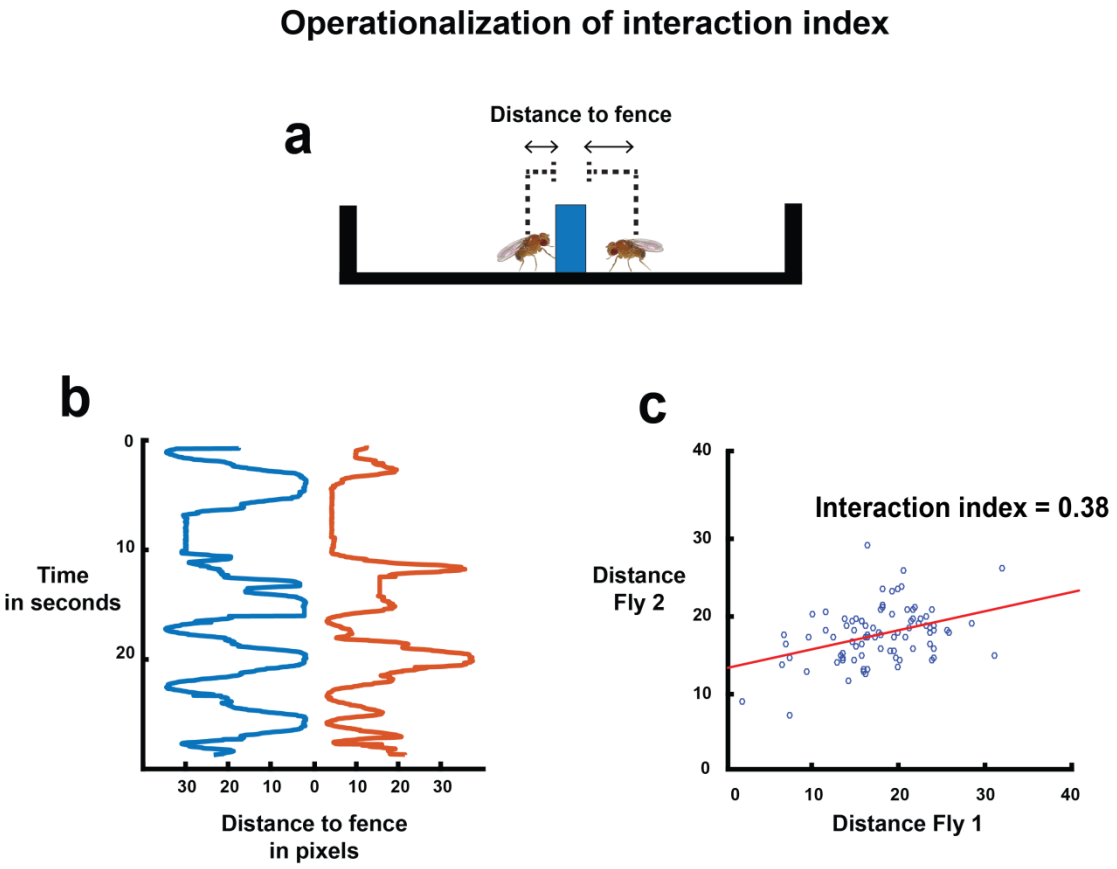

Figure 2. Description of interaction index metric used in analyses of affiliative behavior experiments. **a**: Side-view drawing of an individual arena with dyad flies' distances to the fence are depicted. **b**: Movement tracks of two example flies over time as expressed in their distance to the fence. **c**: Example flies' distances to the fence captured at the same frame plotted against one another. Red line is the least squared line. Interaction index is defined as the correlation between both flies' fence distances across the entire time frame.

Indeed, the fewer sensory modalities affected, the higher the mean absolute interaction index, i.e., the more similar was dyad flies' movement (**Fig. 3**).

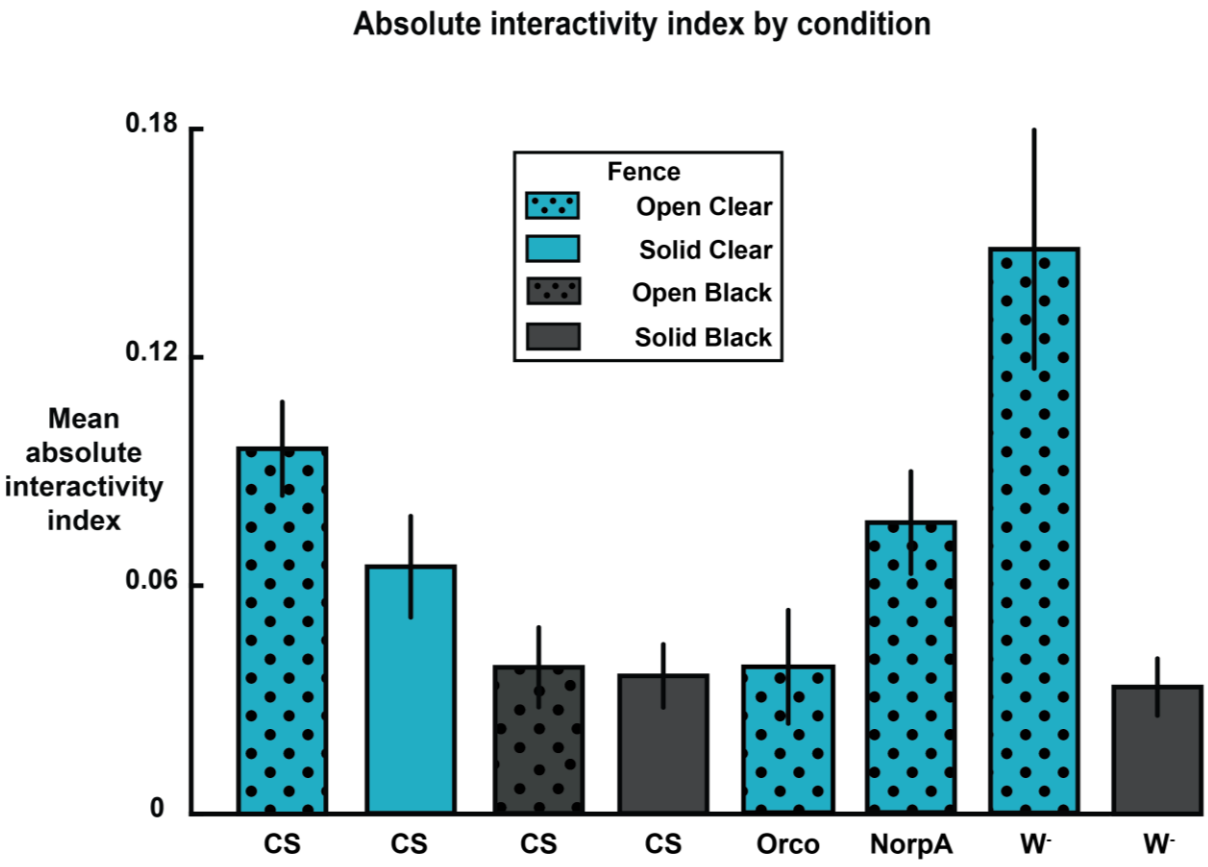

Figure 3. Mean absolute interactivity indices across fence- and genotypes. Error bars denote 95 % confidence intervals. Color and patterns denote type of fences used to separate flies. X-axis describes genotypes.

Differences in affiliative behavior were not caused by differences in speed brought on by increased activity levels when a conspecific was sensed. In fact, mean speed is not affected when a fly is

visible as a dyad-neighbor compared to when the neighboring half-arena is empty, $t(145) = -0.085$, $p = .932$ (**Supplementary Fig. 5**).

Canton-S flies as well as flies in W- background showed significantly higher mean absolute interaction indices when an open clear fence separated flies within a dyad compared to a solid black fence, $t(598) = -4.62$, $p < .001$; $t(132) = 6.35$, $p < .001$, respectively. Interestingly, reducing only visual information flow as opposed to only olfactory information flow led to a significantly less reduced mean absolute interaction index in CS, $t(561) = 1.99$, $p = .046$; $t(556) = 3.59$, $p < .001$. On the other hand, anosmic Orco mutants exhibited a significantly lower mean absolute interaction index compared to blind NorpA mutants, $t(115) = -3.52$, $p < .001$.

Next, we investigated persistence in affiliative behavior within dyads. Besides a dyad's interaction index, we characterized affiliative behavior by the amount of simultaneous coincidental fence approaches between dyad flies. A 'coincidental approach' refers to both flies in a dyad coincidentally moving within one body length (3 mm) of the fence (**Fig. 4**).

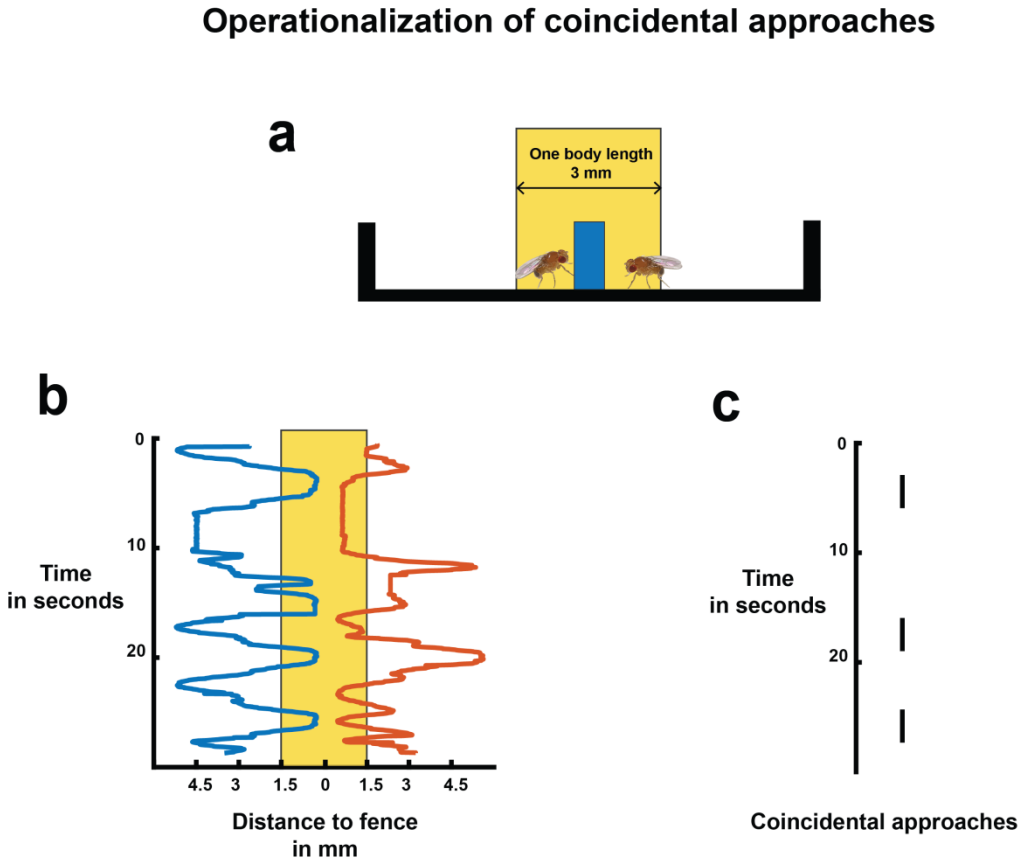

Figure 4. Description of coincidental approach metric used in analyses of affiliative behavior experiments. **a**: Side-view drawing of an individual arena with approach area shown in yellow. Coordinates of the area borders were used to score coincidental approaches. **b**: Movement tracks of two example flies over time as expressed in their distance to the fence in millimeters. Yellow area corresponds to approach area shown in **a**. **c**: Example flies' coincidental approaches over time. Coincidental approaches shown correspond to movement tracks depicted in **b**.

We observed a significant day-to-day correlation in the number of coincidental approaches within CS dyads with an open clear fence over 6 days (**Fig. 5**). Since this correlation ceased to show significant differences from 0 when flies were randomly shuffled across dyads, we can assume that the number of

coincidental approaches is persistent within the flies comprising a dyad. Further, as the correlation in coincidental approaches between days is significantly lower within CS dyads with a solid black fence, NorpA, and Orco mutants compared to CS dyads with an open clear fence, we can conclude that sensory information flow is necessary to establish persistence in affiliative behavior dependent on behavior of the other fly in the dyad.

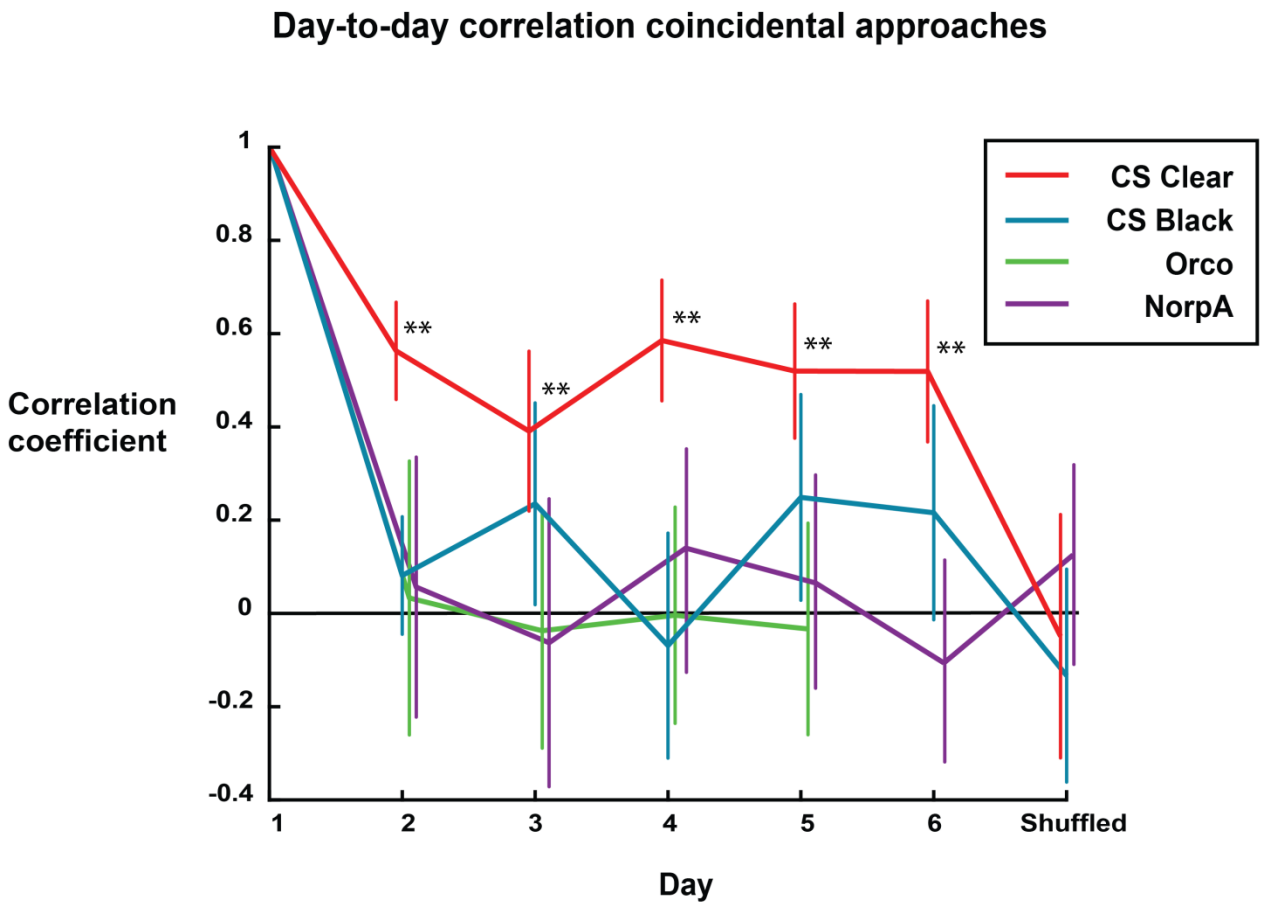

Figure 5. Day-to-day correlation of coincidental approaches within individual dyads over 7 days across fence- and genotypes. *Shuffled* denotes that individual dyads were formed with random flies instead on the 7th day. Colors denote different genotypes and different fences used in wild-type CS groups. *CS Clear*: Canton-S flies separated by clear porous fences. *CS Black*: Canton-S flies separated by solid black fences.

Orco: Orco mutant flies separated by clear porous fences. *NorpA*: NorpA mutant flies separated by clear porous fences (*: Correlation significantly different from 0 with $p < .05$. **: Correlation significantly different from 0 with $p < .001$).

We further determined that affiliative behavior remains stable within dyads even when a single fly is part of multiple dyads, i.e. there is persistence in the quality of unique interactions between two individuals, $r = 0.32$, $p = .017$ (**Fig. 6**).

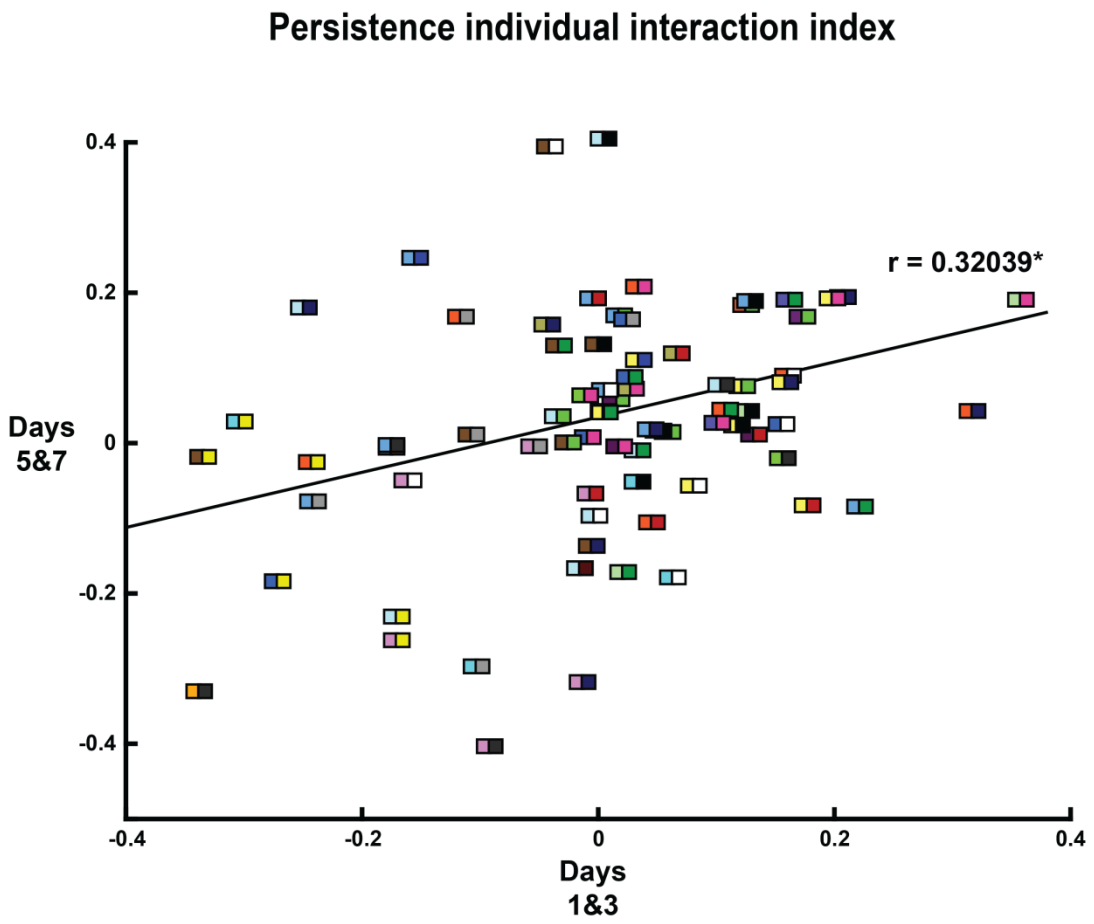

Figure 6. Correlation between first- and second-time iteration interaction indices within individual dyads. *Dyads* were always measured 4 days apart. Rectangles denote dyads. Colored squares denote individuals

forming a dyad. Note that, for example, *left-yellow* and *right-yellow* designate different individuals. Black line is the least squared line. Asterisk denotes significance at 5 % level.

Strikingly, interaction indices in dyads that an individual fly was part of tend to cluster in their magnitudes on both iteration times (**Fig. 7**).

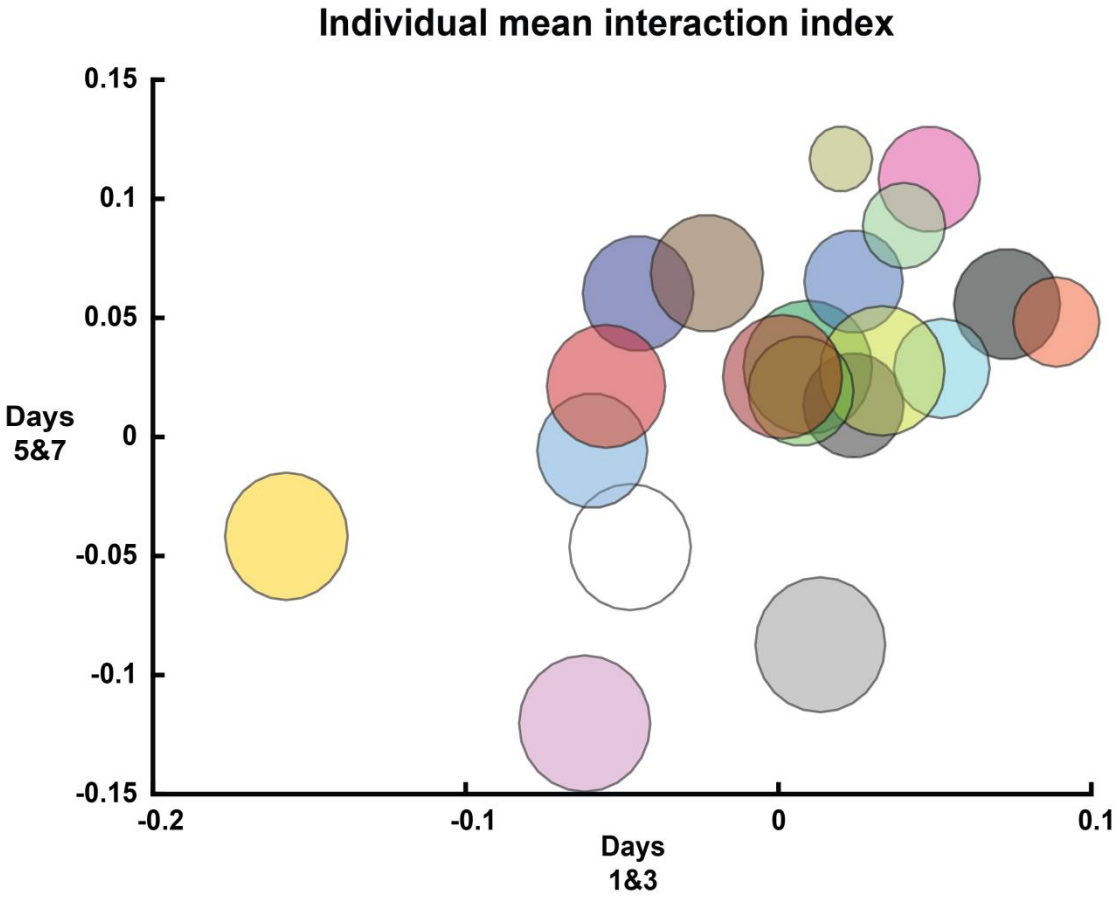

Figure 7. Individual mean interaction indices on two measurement occasions plotted against one another. Circle center corresponds to individual flies' average interaction index across dyads it was part of. Circle radius corresponds to 1 SEM computed using pooled standard deviation across both measurement occasions.

To wit, individual flies appear stable in measures of affiliative behavior across multiple dyads. Indeed, a repeated-measures analysis of variance (RM-ANOVA) revealed a significant main effect of fly identity across measurement times (**Fig. 8**), which suggests evident idiosyncrasy in persistent affiliative behavior, $F(19, 754) = 3.52$, $p < .001$.

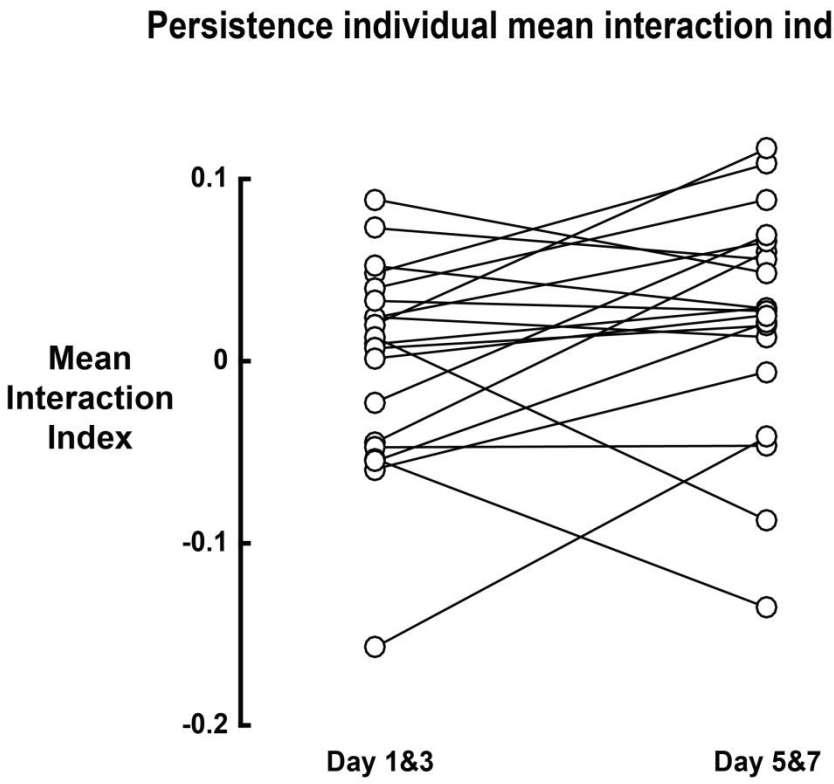

Figure 8. Spread of and change in individual mean interaction indices over time. Overall, individuals change less in their mean interaction index within compared to the differences in interaction indices across individuals.

Last, we constructed a 10 x 10 social interaction network (SIN) by extending the paradigm in such a way that each fly is part of each possible dyad. This setup resulted in 45 unique dyads. Social network structure visually remained persistent over 2 days (**Fig. 9**).

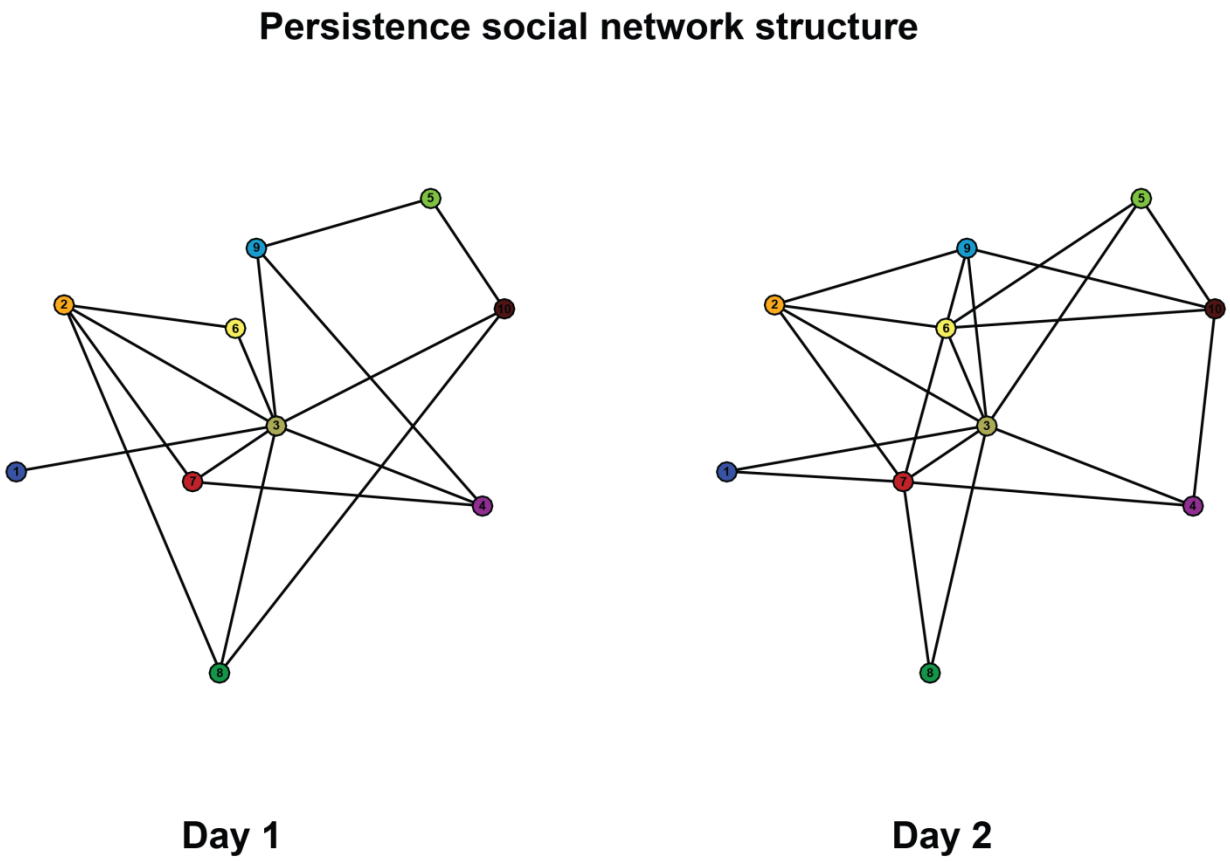

Figure 9. Persistence in social network structure over 2 days. Colors and numbers in nodes differentiate individuals. While the positive correlation of measures of affiliation implies that social networks are stable, SINs typically are represented with binarized edges. Thus, we applied reasonable thresholds to our continuous measures to produce more typical SINs. Connections between nodes denote supra-threshold dyad absolute interaction indices. Same threshold of +/- 0.113 (mean interaction index on first day +1 SEM) was used on both days.

Individual dyads exhibited persistent number of coincidental approaches $r = 0.35$, $p = .009$, as well as interaction indices $r = 0.24$ $p = .034$ (**Fig. 10**). Likewise, RM-ANOVA showed a significant main effect of fly identity on interaction index, $F(9, 280) = 6.14$, $p < .001$, and coincidental approaches across times, $F(9, 304) = 1.56$, $p = .126$. This reaffirms our hypothesis that idiosyncrasies in affiliative behavior remain stable over time.

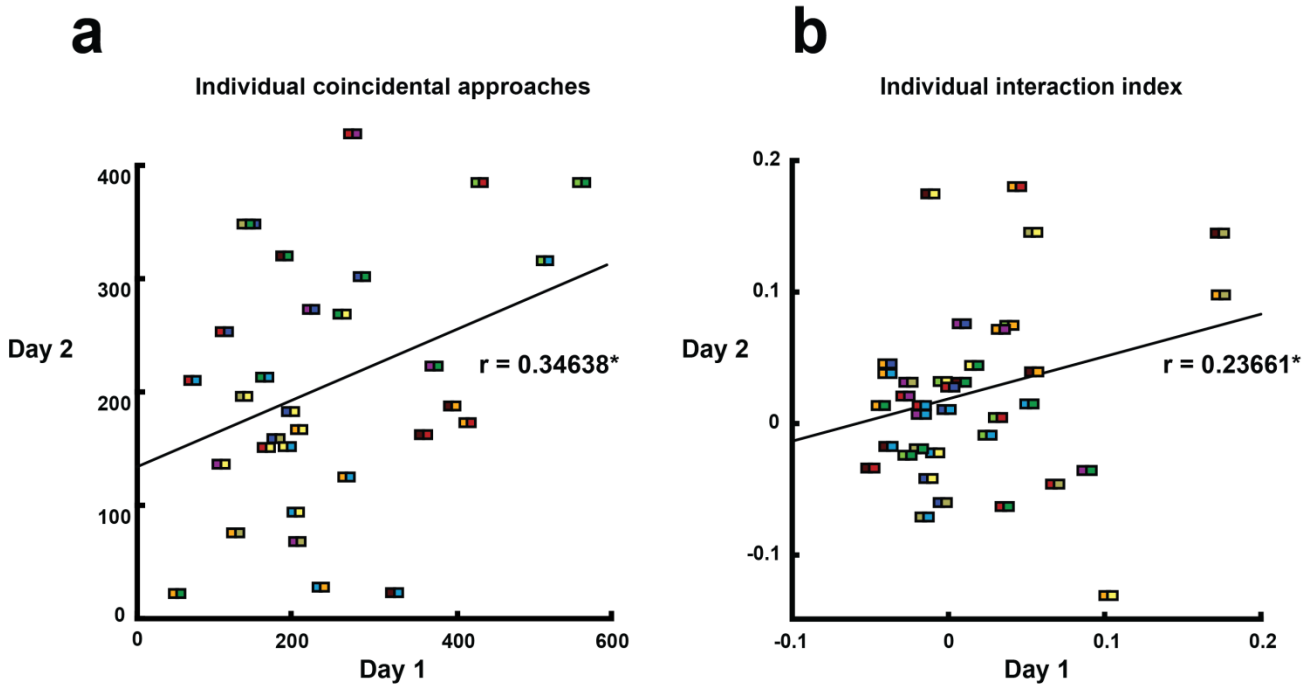

Figure 10. Persistence in individual coincidental approaches and interaction indices across 2 days. Rectangles denote dyads. Colored squares correspond to individuals forming given a dyad. Individual's colors correspond to those in **Fig. 9**. **a**: Correlation in individual coincidental approaches between 2 days. Black lines are least squares lines. Asterisk denotes significance at 5 % level. **b**: Correlation in individual interaction indices between 2 days. Black lines are least squares lines. Asterisk denotes significance at 5 % level.

Robot

We built a custom robot in the style of a 3d printer with Cartesian motion control (X-Y and Z axes). The robot drew design principles and techniques from the DIY/maker community and was therefore inexpensive (all parts together > $1000). The entire robot platform is designed to be modular and to be used in a wide variety of experimental contexts (**Fig. 11**).

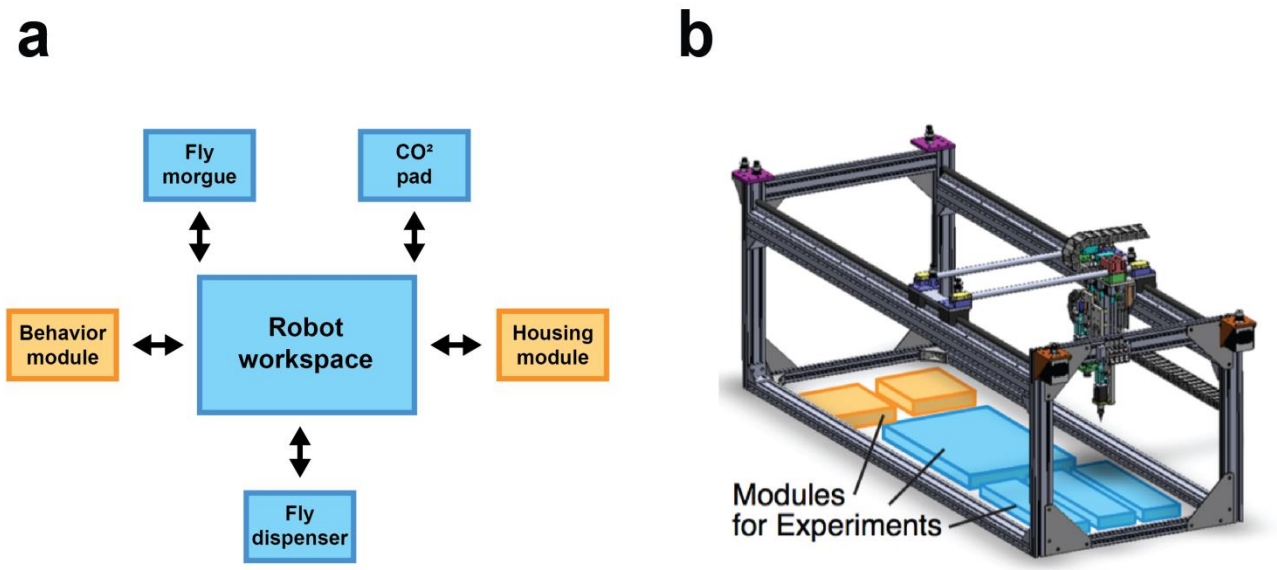

Figure 11. Overview of robot and individual modules. **a**: Schematic of robot workspace and modules. Arrows show possible fly transport. **b**: Drawing of robot platform and modules in spatial relation.

Within one context, modules remain stationary while the robot autonomously moves individual flies between modules (**Supplementary Video 1**). The robot is equipped with a two-motor belt pulley system capable of moving its instruments at high speed (30 cm/s) and accuracy (within 100 µm) over the entire work space (130 x 50 cm^2) in 2 dimensions. End effectors comprise a high-resolution camera, a multi-purpose vacuum part manipulating tool, and a positive/negative air pressure-directing tool for individual fly handling (**Fig. 12**).

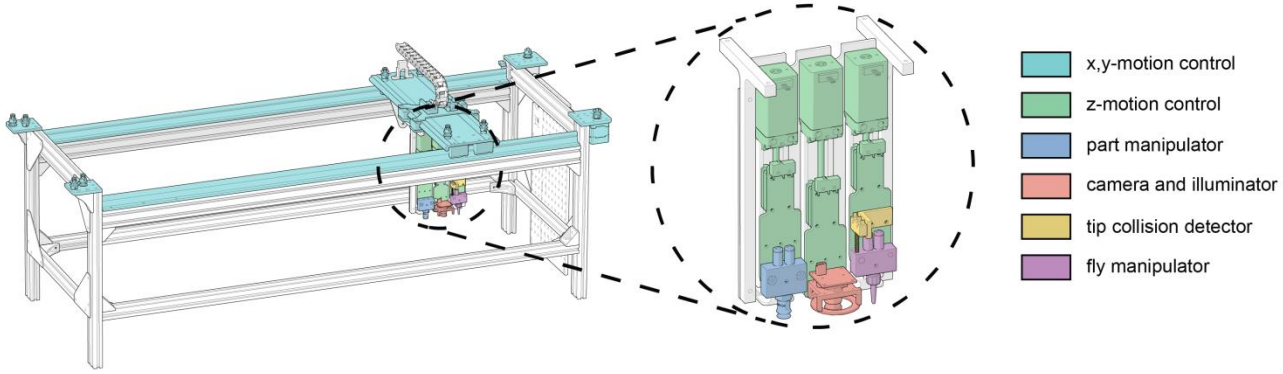

Figure 12. Schematic of the robot and its individual instruments. Belts responsible for x- and y-motion are omitted for visibility. Limit switches (omitted for clarity) are present on the underside of each individual instrument's motor to prevent accidental z-movement damage, as well as on the railing bounds of the robot platform to prevent accidental x- and y-movement damage and allow accurate homing.

Instruments can be individually moved along their Z-axis in precise increments (0.005 mm). Awake flies are gently vacuumed into the individual fly handling instrument (1 N across 3mm² tip diameter) and held in place by a perforated aluminum membrane. Flies are expelled from the fly handling instrument by short bursts of positive air pressure (three 100 ms bursts at 0.1 Ns across 3mm² with 200 ms intervals). Handling flies in this manner did not adversely affect survival rate or activity levels (**Fig. 13**).

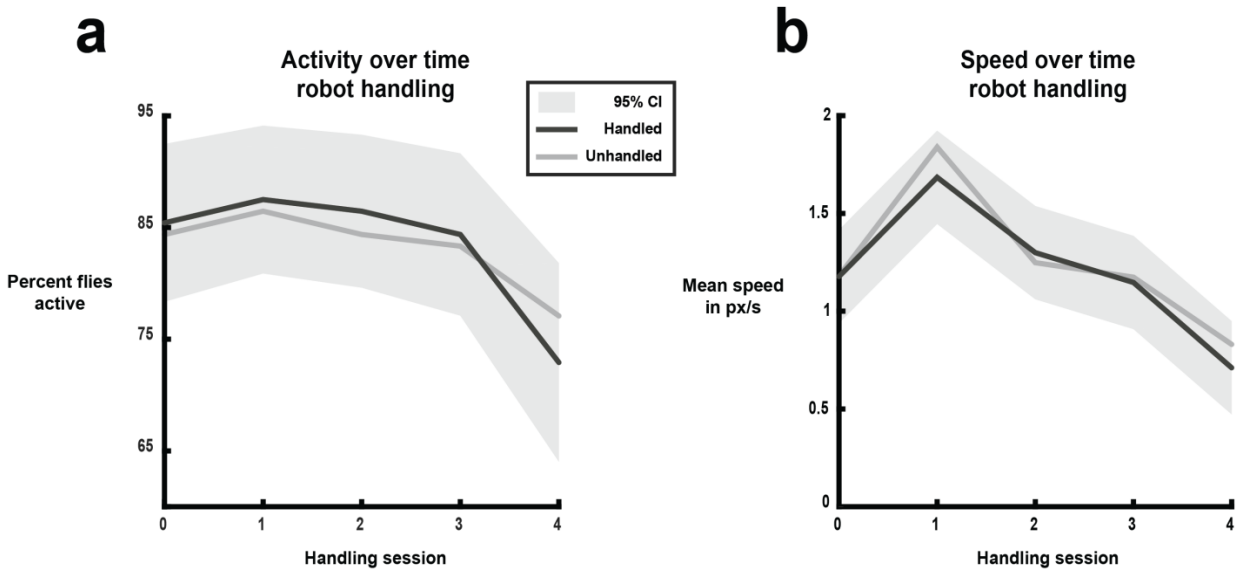

Figure 13. Mean activity and speed comparisons between repeatedly robot-handled and unhandled flies over 5 daily handling sessions. Session *0* was performed directly after first-time robot handling. For visual clarity, only the 95 % confidence interval around handled flies is shown. **a**: Percent flies showing supra-threshold average movement (1 px/s) over 5 one hour sessions. Repeated handling by the robot did not affect the total amount of active flies on any test day. **b**: Mean within-session speed of active flies over 5 one hour sessions. Repeated handling by the robot did not affect the individual mean speed of flies on any test day.

We created a variety of modules for conducting fly experiments that could be implemented into the robot platform. These include a tray with 96 individual arenas used in all affiliative behavior assays here. The robot is capable of moving flies between a 96-arena tray in the behavior module and their individual wells in the housing module in 21.4 +/- 3.7 minutes (s.d.) at 59 +/- 19.3 % accuracy on the first iteration. Missed flies are revisited in subsequent iterations until all flies have successfully been moved or a predetermined time limit has been exceeded. After 5 repetitions, 94.5 +/- 3.2 % of flies are successfully

moved (**Fig. 14**).

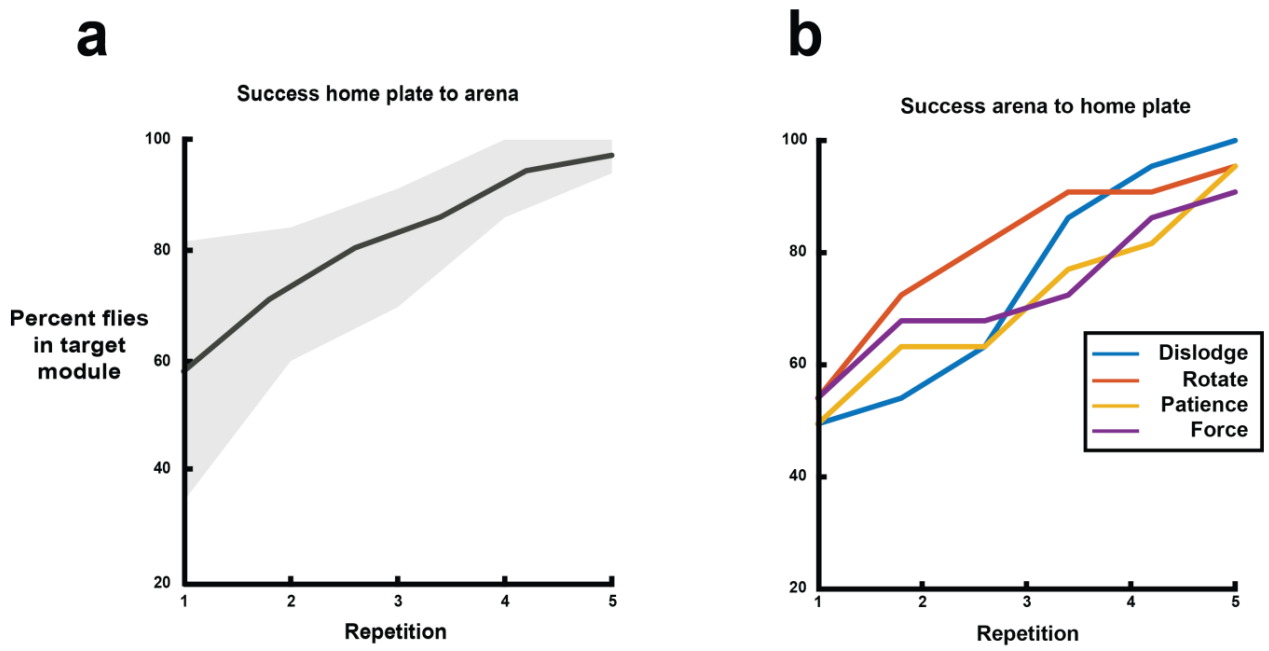

Figure 14. Cumulatively successfully robot-moved individual flies over iterations. **a**: Percent flies successfully moved from housing to behavioral module over time across 10 trials. Gray area denotes +/- 1 standard deviation. **b**: Percent flies successfully moved from behavioral to housing module over time across 4 trials. Colors denote different strategies the robot employed to remove flies from individual arenas (**Supplementary Table 1**).

Subsequent iterations are considerably shorter, depending on the number of missed flies (20.5 +/- 2.1 s per fly). To determine a missed fly, the robot uses machine vision to check for motion in each arena (**Supplementary Fig. 1**). Upon exceeding the time limit, the robot is optionally capable of taking pictures of problematic arenas and sending them to the user via email, who may then instruct the robot to proceed should the pictures reflect false negatives.

We extended the robot's email capabilities to allow remote access functionality. When in an email-receptive 'listening mode', the robot periodically checks for and executes sent commands. Types of command (such as *move flies* or *start virgining*) are preprogrammed with the user specifying variables within the command prompt. An example application might instruct the robot to begin transferring a specific amount of flies from the housing module into the behavioral module after a specific amount of time has elapsed. The robot's remote access capabilities are instrumental for continuous longitudinal experiments that require constant attention and potential adjustments.

To allow handling of awake flies and to decrease individual fly-loading time into individual arenas within the behavioral module, we developed an air-lock mechanism that allows opening and closing of arenas by the individual fly handling instrument directly (**Fig. 15**).

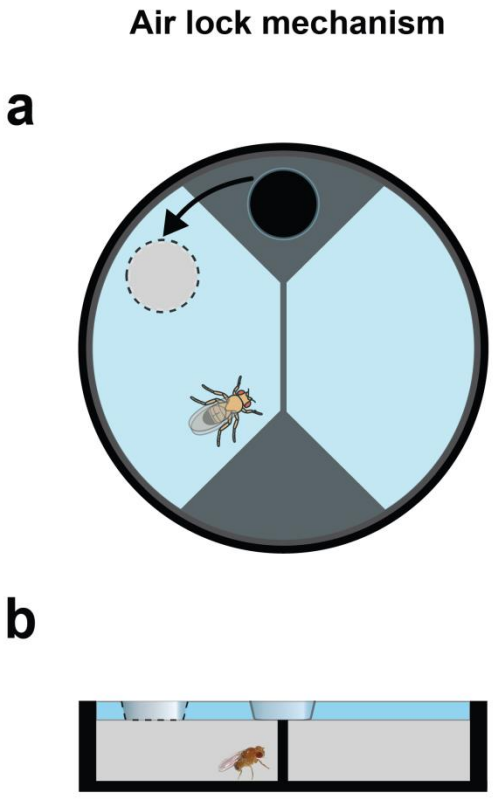

Figure 15. Drawing of the air lock mechanism in individual arenas used in affiliative behavior experiments. One tray constitutes 81 such arenas arranged in a 9 x 9 square. **a**: Top-view drawing of an individual arena. Arrow denotes direction in which to rotate the lid to open the air lock to access the left arena-half. **b**: Side-view drawing of an individual arena. In the starting position, the lid opening is obstructed by the wedge-shaped triangle visible in **a**. Beveled opening edges aid guide the robot's fly handling tip enter the opening.

While a fly is kept in the fly handling instrument, the robot opens the air-lock, releases the fly, and closes the air-lock in discreet steps performed in rapid succession (**Supplementary Fig. 2**). Depending on the starting position of the air-lock opening, the robot loads flies into arenas in 5 +/- 0.6 seconds. To increase versatility with regards to different arena sizes and shapes, the robot utilizes machine vision to detect air-lock openings (**Supplementary Fig. 3**). The machine vision algorithm determines relative opening position in 0.8 +/- 0.06 seconds with 99 +/- 1 % accuracy. We established the success ratio by instructing the robot to 1) find the air-lock opening, 2) enter the opening, and 3) close the opening at a random position repeatedly for 24 hours.

We next demonstrate that flies handled by the robot do not exhibit disrupted complex behaviors. To that end, we compared behavior of flies handled by the robot with that of flies that were handled by a human. We elected to compare two established behaviors, namely circling bias and locomotor handedness (see Buchanan, Kain, & de Bivort, 2015). There was no significant difference between the distributions or mean effects of either behavior in flies handled by the robot compared to a human (**Fig. 16a-d**).

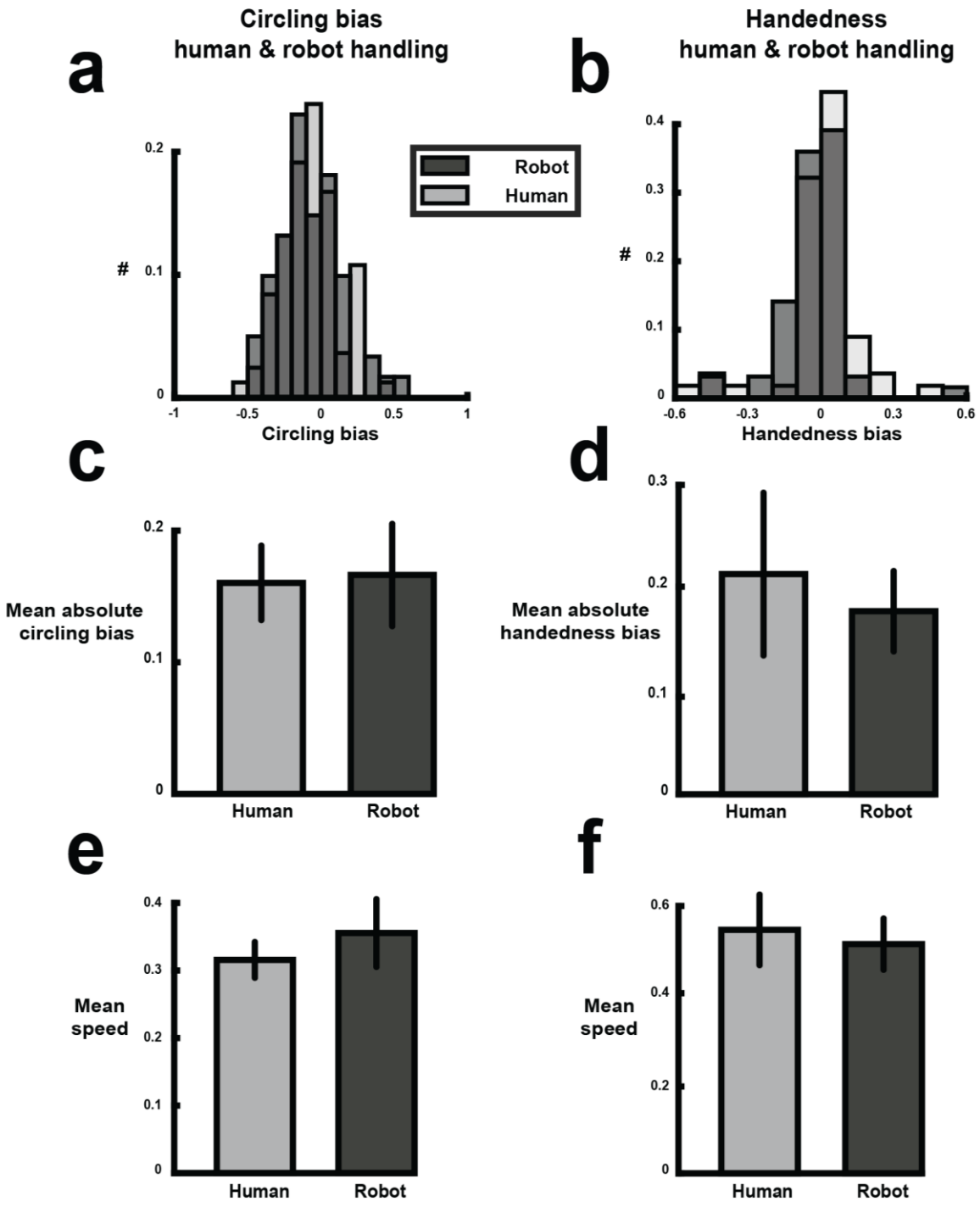

Figure 16. Effect of robot use on established behaviors circling bias and locomotor handedness. Circling bias was assessed in affiliative behavior arenas while locomotor handedness was assessed in y-maze arenas equipped with an air-lock. **a**: Distribution of circling bias (negative means more leftward circling

bias) in robot- compared to human-loaded flies. **b**: Distribution of locomotor handedness (negative means more left turns taken) in robot- compared to human-loaded flies. **c**: Mean absolute circling bias in robot- compared to human-loaded flies. Error bars denote +/- 1 SEM. **d**: Mean absolute locomotor handedness in robot- compared to human-loaded flies. Error bars denote +/- 1 SEM. **e**: Mean speed in robot- compared to human-loaded flies throughout circling bias experiment. Error bars denote +/- 1 SEM. **f**: Mean speed in robot- compared to human-loaded flies throughout locomotor handedness experiment. Error bars denote +/- 1 SEM.

Apparent health of flies (operationalized here as the mean speed throughout the experiment) also did not differ significantly between robot- and human-handled flies in either behavioral assay (**Fig. 16e,f**). Furthermore, long-term persistence in individual circling biases was conserved in robot-handled flies (**Fig. 17**).

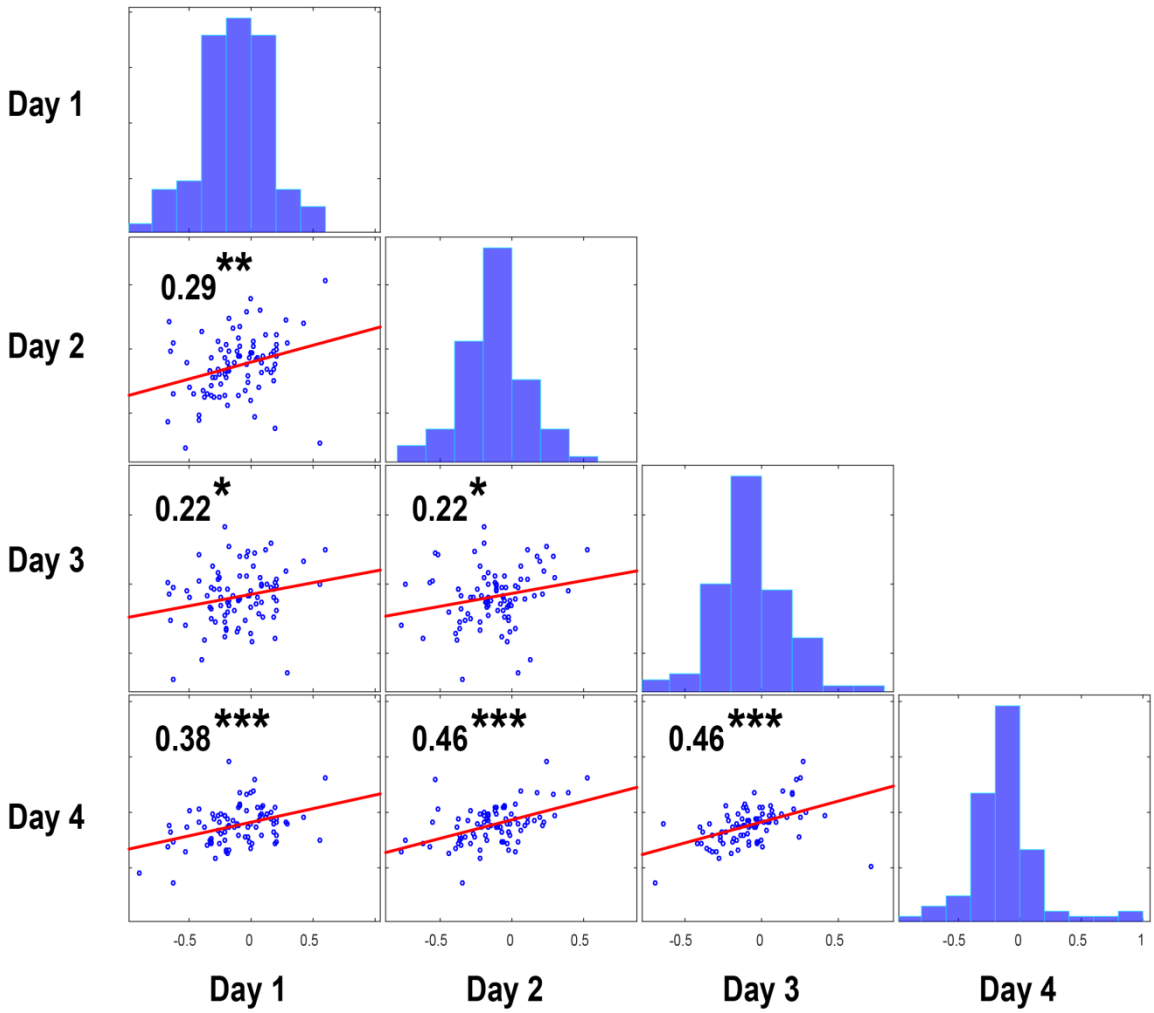

Figure 17. Correlation plot of individual flies' circling bias over 4 days (*: $p < 0.05$, **: $p < 0.001$, ***: $p < 0.0001$).

In summary, using the robot to handle flies has no effect on their general health, does not bias the distribution of individual-to-individual differences, and does not disrupt persistence in established behavioral idiosyncrasies.

Virgining

Whenever only a genotype-specific mating may occur (e.g., when performing a cross), it is important to restrict access to mates of differing genotypes beforehand. This is because female flies may store sperm for days, potentially resulting in offspring of unwanted genotype (Bloch Qazi, Heifetz, & Wolfner, 2003). To this end, virgin females have to be identified and removed from rearing bottles shortly after eclosion, in a process commonly referred to as 'virgining'. Besides its relevance in maintaining accuracy of crosses, virgining is important to reduce known confounds in social behavior. Mated and virgin flies qualitatively differ in various social behaviors, such as aggression and courtship (Nilsen, Chan, Huber, & Kravitz, 2004; Saleem, Ruggles, Abbott, & Carney, 2014). To reduce such confounding factors, it is therefore important to identify flies as virgins when investigating social behavior. Virgining is traditionally done manually, accompanied by the associated time cost. Here, we illustrate that the robot is capable of automated autonomous virgining.

Instead of manually supplying flies into housing or behavioral modules, the robot may additionally interface with an individual-fly dispenser to load newly-eclosed virgins into the work-space modules (**Supplementary Fig. 4**). Raising flies within the dispenser allows for closed-circuit experimental designs using virgin flies that are housed in isolation from eclosion and never exposed to anesthesia (**Supplementary Video 2**). Preparatory steps required to raise robot-born virgin flies are simple and fast, in total requiring 3 +/- 1.5 minutes of additional time per vial. After virgin flies are loaded into individual wells in the housing module, the module may optionally be removed from the work-space for manual sexing. Collecting robot-born newly eclosed flies for two days yields between 62.5 (median: 48) +/- 26.3 flies, 90 +/- 1 % of which were single flies deposited into individual wells (**Fig. 18**).

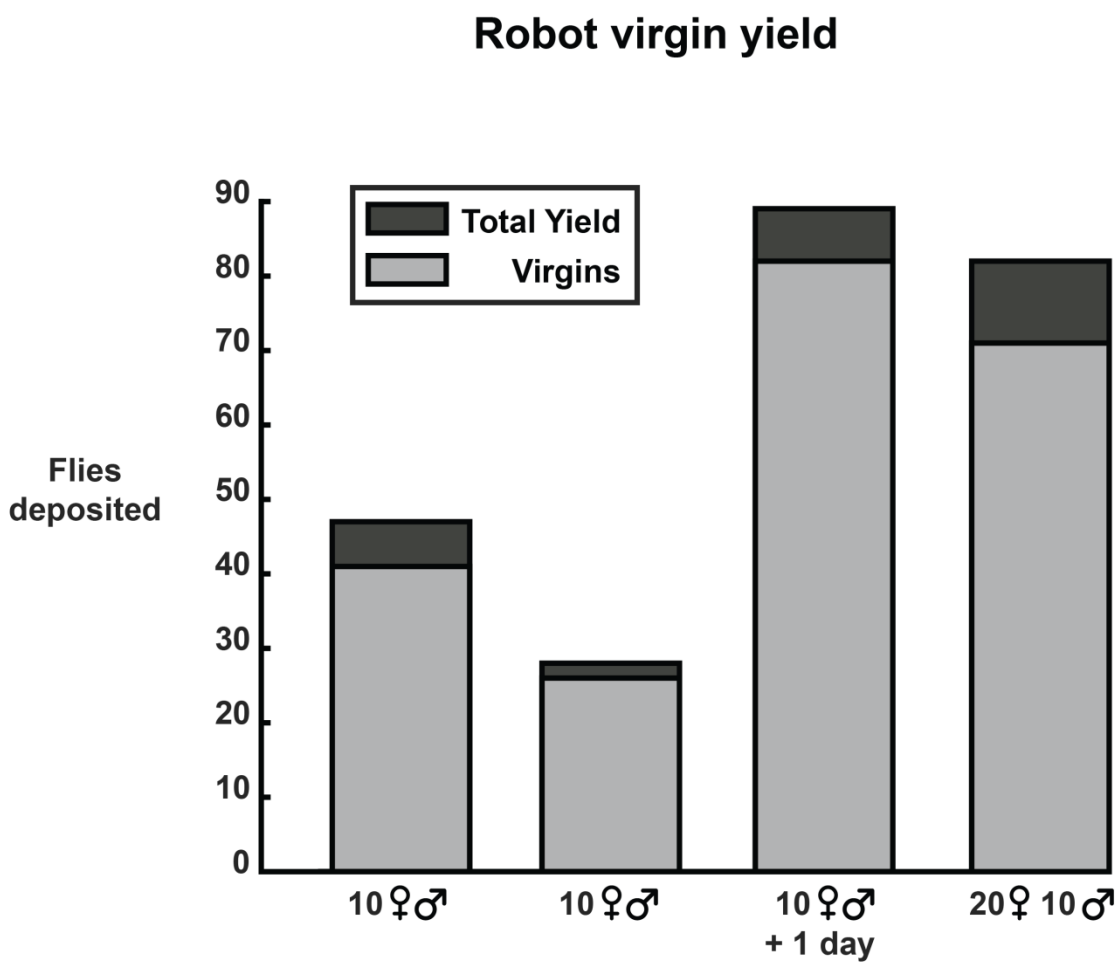

Figure 18. Total flies and virgin flies collected by the robot. Multiple flies deposited in one well are counted as a single non-virgin fly. Symbols and number denote amount and sex of parents placed in the custom virgining vials at the start of the virgining process. Modifier *+ 1 day* describes that the robot continued collection for a 3rd day.

Yield can either be increased by transferring a higher number of female parents into the vial (84 flies total, 86.9 % singly deposited), or by increasing the collection-time (89 flies total, 93.2 % singly deposited). Multiple flies erroneously deposited into single individual wells are easily identifiable and

manually removable. Monitoring agar plates on which singly deposited flies were allowed to oviposit for 10 days revealed a 100% virgin rate (0 larvae or pupae).

Methods

Robot Technical Specifications

The robot comprises 4 linear motion railings on vertical supports with 2 stepper motors on their far ends, 2 rubber belts encircling the robot on 10 pulley cogs attached to the corners of the support railings. The robot's main dimensions including supporting railings are 130 x 50 x 40 cm^3. To improve ease of access, the robot is placed on height-adjustable legs (60 – 90 cm). Cogs attached to the far end of the support railings are also connected to the stepper motors to induce belt motion. The main robot arm is suspended on low-friction mounts guided by and attached to the railings and belt leading in X-direction. Y-motion is achieved by sub-mounts on the main arm and connection to the other belt. Mounts are attached perpendicular to each other to allow for motion in all directions. A drag chain protects cables and positive/negative pressure providing tubes leading from individual instruments attached to the main arm through the support railings into the robot's main electronic processing unit. Vacuum and air pressure providing tubes are further connected to in-house positive/negative air pressure supply. Solenoid valves attached to the main arm regulate air flow and are under control of the main processing unit located outside of the main work space.

The robot's main processing unit is a Smoothieboard v1 microcontroller (part list) running the Smoothieware firmware. The robot is controlled using G-code USB interfacing through Python 2.3 running on Windows 7. Scripts containing the robot's sub-routines were written in Python 2.3. Stepper motors pulling belts in X- and Y-directions ran at 1 A, resulting in a maximum speed of 200 mm/s. Stepper motors controlling Z-direction for each individual instrument ran at 0.75 A, resulting in a maximum speed of 83.3 mm/s. Limit switches were installed on main railings and all other parts that could potentially cause collisions during unrestricted robot movement. Limit switch behavior was rerouted to be under sub-routine control as determined by Python scripts instead of directly influencing and restricting current towards stepper motors in a closed-circuit manner. This allowed setting a 'true

zero'- position on all axes, which significantly improved accuracy in robot movement, as well as usage of precise (sub-millimeter) pre-set coordinates for stationary modules on the work space surface. The work space refers to a 110 x 37 cm^2 clear acrylic plate denoting the maximum possible area that all individual instruments can reach. The work space has holes of equal diameter (50 mm) organized in a grid for easy organization and fastening of individual modules using standard 50 mm screws. The work space is designed to be easily replaceable when a different set of experimental modules is required by a given paradigm.

Modules

Dimensions of experimental modules used here to investigate affiliative behavior, circling bias, and locomotor handedness are 30 x 30 cm^2 (**Fig. 17a**). Individual housing module dimensions are 20 x 40 cm^2. All modules used were rectangular or square in shape. In principle, the maximum allottable space in the work space (4 m^2) can be jointly utilized by as many modules as necessary for the desired paradigm. Additionally, there are no theoretical shape restrictions for individual modules. The individual housing module used here is a 96 individual well plate that was placed on a food tray. Individual wells have a 7 mm diameter and are 20 mm deep. Wells have a wide metal mesh floor that allows feeding but prevents escape. Wells are covered with a tight plastic mesh that prevented escape but allowed the robot's individual fly handling instrument (or a handheld aspirator) to penetrate. Flies had free access to standard cornmeal diet on the food tray placed below. Food was replaced every 2 days to maintain adequate moisture and freshness.

Arenas and Trays

Arenas used for affiliative behavior and circling bias experiments are circular in shape with a 30 mm diameter and a height of 3 mm (**Fig. 17b,c**). Two equally large semicircular arenas are formed by a 1.5 mm thick fence. Two triangular wedges are formed by extending the points where the fence ends meet the outer circle. The wedges are necessary to provide a closing position for the air-lock mechanism.

Arenas are covered by a rotatable clear lid with a 3.5 mm diameter opening through which flies can be deposited into and removed from the individual arenas. We refer to a solid black fence as the outer walls forming the circle continuing to form the inner fence. Other types of fences (open clear, solid clear, open black) refer to individually cut out pieces that can be placed into tightly fitting openings in the middle of the circular outer arena. A tray comprises 81 circular arenas, thus containing 162 semicircular arenas in total. All parts are made from either clear or black acrylic and cut into shape using a laser cutter. Outlines for the individual cut-outs making up an entire tray were produced using Autodesk Inventor and preprocessed with CorelDraw. Individual cut-outs were joined together using Plastruct plastic weld.

Fly Dispenser

The individual-fly dispenser consists of a vial holder connected to a funnel, a stepper motor, two Styrofoam wheels, two light-bridge sensors, and a tube attached to a small 2 mm diameter dispensing tip. The mechanism by which a single fly is dispensed comprises the stepper motor moving the vial holder up and releasing it repeatedly, effectively knocking hatched flies inside the vial towards the funnel. Inside the funnel, if the first sensor is triggered, Styrofoam wheels start turning, separating and moving flies already inside the funnel, as well as preventing other flies from entering the funnel by moving closer together. Once the second sensor located right below the wheels is triggered, positive air pressure is generated using an electronic compressor gently moving the fly along the output tube through the dispensing tip. As positive pressure is travelling through the dispenser the wheels stop moving, causing any excess flies to be transported into a second receptacle. The dispenser can be remotely triggered using G-code sent using Python scripts. The robot is capable of physically interfacing with the dispenser through a hub. The hub is an 8 cm diameter, 4 cm high clear, hollow acrylic cylinder with two 5mm diameter Luer lock plastic syringe tips attached on opposite sides. The dispenser remains connected to the bottom side of the hub, while the robot can precisely move to connect to the top side.

Experimental Procedures

Unless otherwise specified, experiments were performed between 9 A.M. and 11 P.M. On the day of experimentation, virgin flies were anaesthetized using CO_2 and aspirated into individual wells in the housing module. After 2 hours of recovery, flies were loaded into individual arenas by the robot with arenas empty after 2 iterations loaded manually using an aspirator. Flies were later removed from their arenas in an identical fashion. Trays were filled with 162 flies and monitored inside illuminated boxes in a temperature (23℃) and humidity (41%) controlled behavioral observation room. Fly movement was tracked for 1 hour. Fly tracks were analyzed using a custom MATLAB script. To minimize behavioral confounds caused by disparate loading times, one arena-half was filled first. This ensured that flies in arenas that were filled earlier were not allowed more time to familiarize with their dyad-neighbor. Two flies present in the same arena separated by any fence type are referred to as a 'dyad'.

Paradigm validation.

All experiments were conducted in concordance with the general experimental procedures. In total, 972 wild-type CS flies were tracked in open clear fence, 648 CS in solid black fence, and 162 flies in all other conditions (solid clear CS; open black CS; open clear Orco, NorpA, & W-; solid black W-). Order of experimentation was randomized after 4 and 3 trays of flies in open clear and solid black fence conditions, respectively, were analyzed. Since there was no observable effect of sex-composition in a dyad on affiliative behavior in the first 7 observation sessions, sex was not controlled for. Fences were changed after flies were removed from trays directly after tracking.

Day-to-day single dyad persistence.

On the first day of observation, procedure was identical to the general experimental conduct. Instead of disposing flies, however, they were placed back into their individual wells in the housing module. On following days, individual flies were placed into different arenas to prevent confounding factors introduced by arena differences. The same 2 flies formed a dyad on each day except for the 7^{th}. Starting from the 2^{nd} day, flies were not exposed to any form of anesthesia. Food tray placed underneath

the housing module was replaced every 2 days. Time of experimentation across days was held approximately constant. On the 7th and last day, dyads were shuffled, i.e., dyads were broken up and instead formed by flies chosen at random. NorpA and Orco groups consisted of 1 tray à 81 dyads while both CS conditions consisted of 3 trays à 243 dyads each.

20 x 10 multiple dyad round-robin.

Persistence in affiliative behavior of 200 dyads formed by 20 flies was assessed in a similar approach as day-to-day persistence. Instead of once, the tray was monitored 5 times each day for 4 days in total. Dyad composition and order of observation were randomly determined beforehand. Each of the 20 female virgin flies was represented in 10 dyads formed with 10 other flies. All resulting 10 dyads were observed sequentially over 2 days. The second observation of the same dyad took place 2 days after the first observation. Second observations of the same dyad were performed with dyads placed in a random different arena compared to the 1st observation. This prevented arena identity or location confounding with dyad effects on measurements. After 1 hour of observation, flies were returned to their individual wells for 1 hour and allowed to recover and feed. They were then paired with their next predetermined dyad-neighbor and observed for one hour. This continued until each fly was observed in 5 different dyads.

10 x 10 social interaction network.

Persistence in individual affiliative behavior and social network structure was assessed similarly as the 20 x 10 round-robin experiment. All flies used were born in the dispenser, never exposed to anesthesia, and never handled manually. All flies were female and virgins, as was determined by examining the first used food plate for larvae for 10 days. Each of the 10 flies was prearranged to form a dyad with every other fly constituting what will be referred to as a social interaction network (SIN). After 1 hour of observation, flies were allowed to rest for 30 minutes. Shortening resting period in the housing module allowed all possible dyads to be observed on the same day.

Virgin yield.

Ten male and 10 (20) female CS between 5 and 7 days post eclosion are placed in custom dispenser-type vials. Vials are 10 cm long at a 4 cm diameter with a detachable bottom container part. Standard cornmeal diet is poured in the container and allowed to cool down prior to fly introduction. Flies are anaesthetized using CO_2 and placed in the vial. After 2 days in the incubator (25°C), flies are discarded and the vial is placed back in the incubator. After 9 days, food is removed from the container, the container thoroughly washed and reattached to the vial. The vial is placed into the dispenser and the virgining robot's virgining subroutine is engaged. Over the following 2 (3) days, the robot loads newly hatched flies into individual wells in the housing module. Total yield is defined as individual wells in which at least one fly is loaded. Singles are defined as wells in which only one fly is loaded. Wells in which more than a single fly is placed are manually emptied. The remaining flies are kept in their individual wells for 10 days. The housing module and food tray are removed and placed inside a sealed plastic container. Last, the food tray is examined for larvae, eggs, and newly hatched flies. If none can be found, single flies placed into individual wells by the robot are considered virgins.

Robot handling effect.

Ninety-six 5-day old flies were aspirated into individual wells in the housing module and allowed 30 minutes recovery time. The robot then started repeatedly vacuuming out and depositing back in each fly 10 times in a row. The housing module was then placed under automatic observation while fly movement was tracked. Afterwards, we repeated the same steps using a fresh batch of flies without engaging the robot as a control condition. Flies in the control condition were allowed to rest for the same amount of time as the robot required handling each fly in experimental condition. We used a custom MATLAB script to determine flies' mean speed. We also determined how many flies died after each observation session manually. The entire session was repeated 5 times in total.

Measurements and Analyses

Flies' movement was tracked using a custom real-time MATLAB script interfacing with a Firefly MV FMUV-13S2C USB-camera. Tracks were analyzed in MATLAB. A mean speed and distance-travelled threshold was applied to remove immobile flies from analysis. On average, five flies per 162 arena tray were removed in this way (~ 3%). Tracks were first transformed into coordinates relative to the half-arena in which the fly was placed (**Fig. 1c**). Next, distance between the fly centroid and the fence on each frame (29.9 fps) was determined. Interaction index of a dyad was determined as the correlation in distances to the fence between both flies across the experiment. An interaction index of ~ 0 reflects either random movement across both flies or one fly moving and the other fly remaining immobile. If both flies remained immobile, the speed threshold would have removed the dyad. A positive interaction index reflects one fly approaching the fence while the other fly increases its distance both to the fence and the other fly. A negative interaction index reflects both flies being located close or far away from the fence at similar times.

A coincidental approach refers to both flies being within 0.5 body-lengths (1.5 mm) of the fence at the same time. Once a coincidental approach is detected, the next approach is only scored if one of the flies moves further than 0.5 body lengths away from the fence for more than 2 seconds. Since coincidental approaches are sensitive to differences in speed (as opposed to interaction index), they are corrected by the dyad mean speed (the mean of each dyad's fly's mean speed) in pixels per frame. Speed in pixels per frame was approximately normally distributed with a mean of 0.15 and a standard deviation of 0.06 across individual flies.

Connections shown in **Figure 9** represent all dyads in which specific individuals exceeded an interaction index of the tray mean +/- 1 SEM on the first observation day. The same threshold value was applied to visualize connections on both days. Threshold value does not coincide with the largest threshold-dependent day-to-day degree correlation coefficient possible given the presented data (**Fig. 19**).

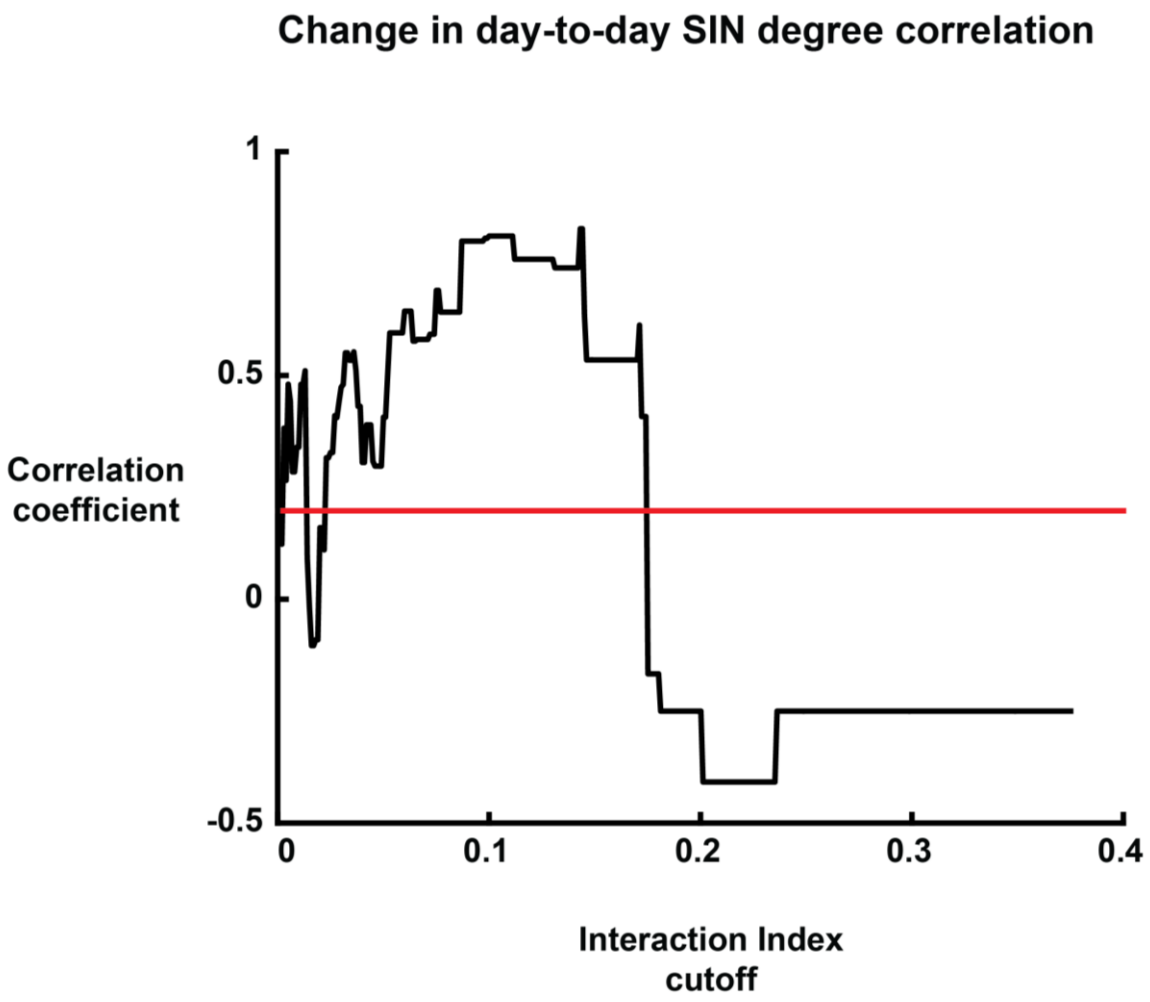

Figure 19. Effect of interaction index cutoff on day-to-day correlation between network degrees. Red line represents critical Z-score cutoff at which correlation coefficient is significant at $\alpha = .05$.

A network's degree refers to the total number of connections between flies. We chose the threshold in such a way that a maximum amount of connections are retained after thresholding. As seen in **Figure 19**, thresholding in a way that at least 1 connection remains on the first day (interaction index threshold below 1.8) results in a sweep of significant, moderate-high correlation coefficients. Correspondingly, applying only a very low threshold (above 0.019) results in a similar set of moderate-high correlation coefficients. Note that no or very little thresholding would have biased the correlation

coefficient as more flies were alive and active on the first day compared to the second, i.e., the total number of possible connections would not have been balanced.

Fly Lines

All experiments were performed using Canton-S (wild type), *Orco*, *NorpA*, and/or w^{1118} lines. Mutant lines were homozygous. We raised flies on standard cornmeal diet (Jazz-mix Drosophila food, Fisher Scientific, Pittsburg, PA, USA) under 12 h/12 h light and dark cycle in an incubator at 25℃ and 70% humidity. Virgin flies were collected using carbon dioxide (CO_2) and housed in vials of 15 to 20 flies, unless otherwise specified. Five days post-eclosion, flies were transferred into individual wells in the housing module using CO_2 and used for experimentation after 2 hours of recovery.

Discussion

Here, we presented an individual fruit fly-handling robot capable of unsupervised closed-circuit high-throughput experimentation. The robot is designed to be modular (**Fig. 1**) and usable in a variety of different experimental contexts. The robot's footprint (130 x 50 x 40 cm^3) and price (all parts together < $1000,-) are minimally restrictive. We demonstrated that robot handling neither harms flies (**Fig. 13**) nor alters their behavior (**Figs. 16 & 17**). Individual flies are handled accurately and transported rapidly between modules (**Fig. 15**). The robot is capable of autonomous virgining (**Fig. 18**) and subsequent closed-circuit integration of virgins into existing paradigms (**Supplementary Fig. 4**).

In order to demonstrate the robot's potential, we developed a novel paradigm for the investigation of persistence and idiosyncrasy in affiliative behavior, as well as social interaction networks (SINs) in *Drosophila melanogaster*. We quantified affiliative behavior by analyzing movement of fly pairs (dyads) separated by different types of fences (**Figs. 2 & 4**). Social networks are then formed based on thresholded measures of affiliative behavior. Instead of imputing concrete interactions between individuals in a group within a time frame (Pasquaretta et al., 2016; Ramdya et al., 2014; Schneider et al., 2012), this assay can be used to describe differences in idiosyncratic affiliative behavior, as well as distinct relationships between individuals. This approach is based on common analyses of human social networks (Contractor & DeChurch, 2014; Kossinets, 2006). Whereas the traditional concrete approach captures information flow under specific temporal and spatial circumstances, the abstract approach attempts to describe the general potential for information flow. Importantly, potential for information flow between individuals is relevant principally when it is not entirely random or exclusively environmentally dependent. In other words, prediction of individuals' future behavior is viable only when behavior is both idiosyncratic and persistent.

In 4 experiments, we demonstrated that 1) fruit flies exhibit persistent idiosyncrasies in affiliative behavior and 2) measures of affiliative behavior can be used to create social networks persistent in

structure. First, we established validity of our paradigm and operationalization (**Fig. 3**). We showed that restricting sensory information flow within dyads either by way of mutant lines dysfunctional in sensation or different fence types diminishes affiliative behavior. Loss-of-function mutations in the no receptor potential (NorpA) gene of *Drosophila* lead to complete elimination of the light-evoked photoreceptor potential, effectively rendering the fly blind (McKay et al., 1995). NorpA mutants used here have previously been shown to exhibit disrupted network structure (Schneider et al., 2012) and impaired social distance modulation (Simon et al., 2012). The *Drosophila* odorant receptor co-receptor (Orco) is essential for the response of tuned odorant receptors to specific odors (Turner et al., 2014). Loss-of-function mutation of the corresponding gene leads to broad dysfunction in olfactory sensing (Larsson et al., 2004). Importantly, sensing male pheromone 11-cis vaccenyl acetate (cVA) is impaired. The pheromone has been implied in numerous social behaviors, such as courtship, aggression, and aggregation with conspecifics (Billeter & Levine, 2015; Ronderos & Smith, 2010). Interestingly, even though Orco mutants similarly exhibit social network structure dysfunction, they were not shown to exhibit differences in social space. This indicates that although our assay utilizes simple measurements of fly movement, it permits capture of more complex social behavior.

Second, we demonstrated that wild-type dyads without sensory constraints, i.e., neither by physical barriers nor by mutations, exhibit persistent affiliative behavior over 6 days (**Fig. 5**). As expected, wild-type flies restricted in visual and olfactory cues about their dyad neighbors by way of a solid separating fence did not exhibit persistent affiliative behavior. Orco and NorpA mutants similarly did not remain persistent in their affiliative behavior between any two subsequent days. This is in line with results of our first experiment. Within single experimental sessions (~ 1h), persistence in SIN structure, and by extension social behavior in general, has been described before (Schneider et al., 2012). Here, we propose that affiliative behavior remains persistent over multiple days.

Third, we showed that affiliative behavior remains persistent when individuals are part of multiple dyads (**Fig. 6**). This suggests that individual flies tend to exhibit a similar magnitude of affiliative behavior regardless of dyad pairing (**Fig. 7 & 8**). In turn, this indicates persistent individual-to-individual differences in affiliative behavior. Last, we showed that social networks can be constructed using thresholded measures of affiliative behavior (**Fig. 9**). In agreement with the previous experiment, we replicated significant day-to-day persistence and idiosyncrasies in measures of affiliative behavior (**Fig. 10**). While there was an overall increase in network degree mediated by a significant increase in magnitude of affiliative behavior measures, characteristic SIN parameters remained stable over both days of experimentation. The fly (node) with the largest influence over potential information flow (i.e., the highest degree, closeness, betweenness, and eigenvector centralities) was the same individual on both days. Similarly, the shortest path possible within the network, a measure of information flow efficiency, passed through the same nodes and was the same length on both days. Overall, although not unequivocal, social network structure parameters here appeared stable over two days.

Persistent idiosyncratic behavior

Persistent idiosyncrasies across numerous different behaviors in *Drosophila melanogaster* and other arthropods have already previously been established. For example, *Acyrthosiphon pisum* displays population-level variability in predator-avoidance behavior (Schuett et al., 2011). Interestingly, behavioral biases were not heritable, suggesting control neuronal circuitry or morphology outside of genetic regulation. In fruit flies, likewise, stable individual differences in circling direction (**Fig. 17**) and left-right locomotor bias have been found to be under control of columnar central complex neurons (Buchanan et al., 2015). Similarly, phototactic behavior (approach-avoidance; photopositivity-photonegativity) constitutes a persistent non-heritable idiosyncratic behavioral trait (Kain et al., 2012). To our knowledge, however, this is the first time *Drosophila* social behavior has been established as idiosyncratic and persistent.

We posit that individual differences in affiliative behavior described here constitute variance in behavioral outputs brought on by idiosyncrasies in internal states, as opposed to a 'social personality' reliant on conspecific identification, recognition, and memory. Internal states can be defined as stored integrated contextual and self-referential information that potentially bias behavior long-term (Gibson et al., 2015). For example, flies may cease avoidance behavior in response to an aversive stimulus if their behavior does not lead to an advantageous outcome (Yang, Bertolucci, Wolf, & Heisenberg, 2013). Importantly, this change in behavior persists longer-term and can be modulated by altering outcome information, e.g., by modifying probability or valence of outcomes in response to avoidance behavior. This suggests that not all behavior is necessarily reflexive but may instead be modulated by experience and context-sensitive constantly-updating internal states. Strikingly, when a group of flies is subjected to repeated predator-like stimuli, such as a moving overhead shadow, a nonsignificant minority persistently exhibits freezing behavior as opposed to the more common avoidance behavior (Gibson et al., 2015). This is interesting insofar that change in response behaviors was still under internal state modulation. With time and repeat exposure, previously freezing flies exhibited more escape behavior. This suggests that changes in internal states can lead to categorical changes between qualitatively different behaviors. In a similar vein, the tendency of individual flies to affiliative more or less with other flies (or, in fact, avoid them) could plausibly be governed by an internal state that is biased in either direction on an individual level. This assumption permits a probabilistic account of affiliative behavior. In other words, depending on a flexible but idiosyncratically biased internal state, individual flies may be more or less likely to engage or avoid a conspecific.

Limitations of paradigm

There are several limitations and drawbacks to the paradigm presented here. First, adopting an abstract approach to social interaction networks renders interpretation of connections and nodes more difficult. Whereas in traditional, concrete approaches connections between nodes can be described as actual interactions between individuals, connections within the abstract approach allude to the quality of

or potential for information passing between connected individuals. In other words, whereas the concrete approach ad-hoc describes interactions between individuals during a particular time frame, the abstract approach taken here attempts to generalize from observed to future potential interactions.

Second, the paradigm is not adapted to allow dyad neighbors to come in close physical proximity. In effect, mechanosensation is heavily impaired. Especially for intact social (Ramdya et al., 2014) and courtship behavior (Billeter & Levine, 2015), mechanosensation is necessary in *Drosophila*. The main issue is manufacturing of suitable fences. All fence types used here are acrylic and lazer cut in shape to facilitate creation of large number of fences at once. A potential remedy would be manual fabrication of acrylic fences interleaved with fine elastic threads allowing partial traverse of the fence by flies.

Third, flies are housed in isolated individual housing wells to maintain identity across experiments. Isolated rearing as a form of altered social experience could affect affiliative behavior. At least SIN structure, however, does not appear sensitive to isolated rearing (Schneider et al., 2012). SIN structural parameters were not significantly different between flies either housed socially enriched or housed in isolation. Even though isolated rearing may not have an effect on SIN structure, social experience is reported to modulate courtship behavior (Billeter & Levine, 2015). It is therefore important to acknowledge a potential confound in future adapted assays.

Robot and anaesthetization

A potentially substantial advantage of using the robot described here is its capability to transport awake flies between housing and experimental areas. Commonly, flies are anesthetized to facilitate manual fly transport between housing bottles and behavioral assays. However, anesthesia using CO_2, cold, or general anesthetics has been found to reduce flies' life span (Perron, Huot, Corrivault, & Chawla, 1972) and disrupt flies' metabolism (Colinet & Renault, 2012). Further, severe impairments in, for example, modulation of social space (Burg, Langan, & Nash, 2013), climbing behavior (Bartholomew et al., 2015), and aggressive sexual competition behavior have been described (Trannoy, Chowdhury, &

Kravitz, 2015). Due to the potential broad negative effects of anesthetization, our robot has the capacity to reduce anesthesia-related behavioral confounds in numerous assays.

Future directions

The robot's core functionalities, namely autonomous handling of awake flies, automatic virgining, and closed-circuit high-throughput longitudinal experimentation can be of use in many different paradigms. Due to its relatively small cost, footprint, and general utility, adopting the robot has the potential to facilitate assaying of widely different behaviors in laboratories with many distinct foci. Further, our novel social behavior assay presented here begets the possibility to investigate potential neural and genetic correlates of idiosyncrasies in affiliative behavior in fruit flies. Due to the robots high-throughput capabilities in combination with the novel assays sensitivity to impairments in affiliative behavior, our automated paradigm can be readily adapted to perform phenotypic screening for affiliative behavior dysfunction.

In addition to the possibility of investigating neural correlates of behavior, the robot's capability for streamlined behavioral screening could potentially be applied to the discovery of pharmaceutical agents. Automated high-throughput screens have already successfully been developed with the purpose of streamlining drug discovery in *Drosophila melanogaster* (Giacomotto & Ségalat, 2010; Pandey & Nichols, 2011; Whitworth, Wes, & Pallanck, 2006). However, most platforms are designed to assess dysfunction or rescue of specific behaviors, such as locomotion or negative geotaxis (Gargano, Martin, Bhandari, & Grotewiel, 2005). Due to its modular design, the robot presented here could be utilized to screen for effects of pharmaceutical agents on a wide variety of different behaviors.

In summary, we created an individual fly-handling robot capable of unsupervised virgining and closed-circuit high-throughput experimentation. Here, we demonstrated the robot's potential in a novel paradigm for the investigation of persistence and idiosyncrasy in *Drosophila* affiliative behavior, as well as social interaction networks. Using the robot to autonomously run longitudinal social behavior assays, we found that 1) *Drosophila melanogaster* exhibit persistent idiosyncrasies in affiliative behavior, 2)

affiliative behavior is diminished with impaired visual or olfactory inputs, 3) persistence in affiliative behavior requires olfactory and visual inputs, and 4) social interaction network structure is topologically stable over time.

Appendix

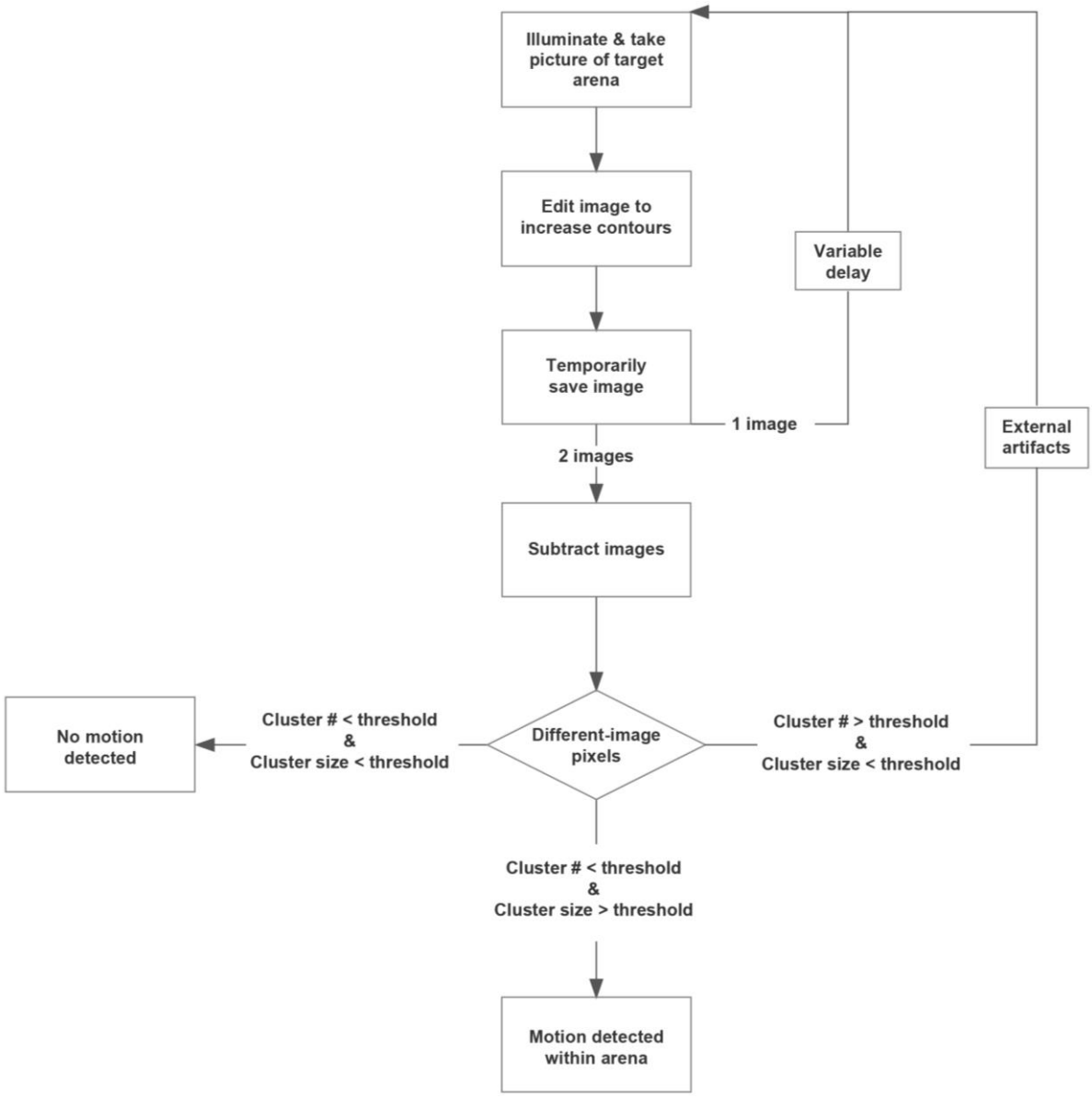

Supplementary Figure 1. Flow chart of algorithm used for motion detection in individual arenas. Variable delay was set to 1 second during all other relevant routines described here. Note that the image editing step includes black-white color transformation. A cluster is defined as column- and row-wise neighboring pixels (1s) in the different-image matrix. Cluster number threshold was set to 2 to accommodate reflections. Cluster size was fixed at 50 pixels, corresponding to an actual sized patch of 0.5mm.

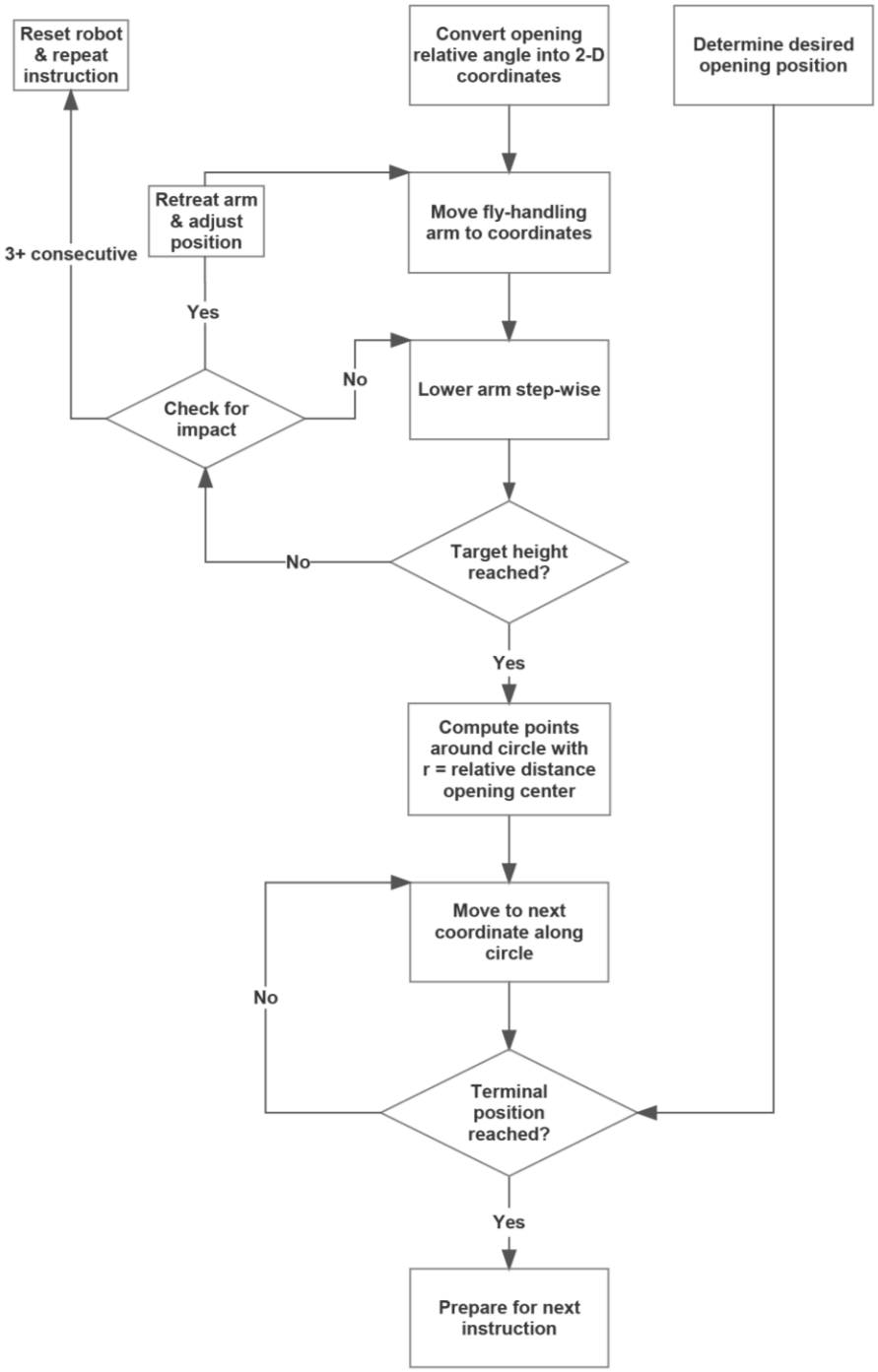

Supplementary Figure 2. Flow chart of sub-routine used to move individual arena lids in a rotary fashion. *Determine desired opening position*: Depending on the scheduled fly position in the arena (left or right arena-half) and current opening position, terminal position either 20, 160, 200, 340 degrees. Degree with the shortest distance to current opening position is chosen to reduce travel-time.

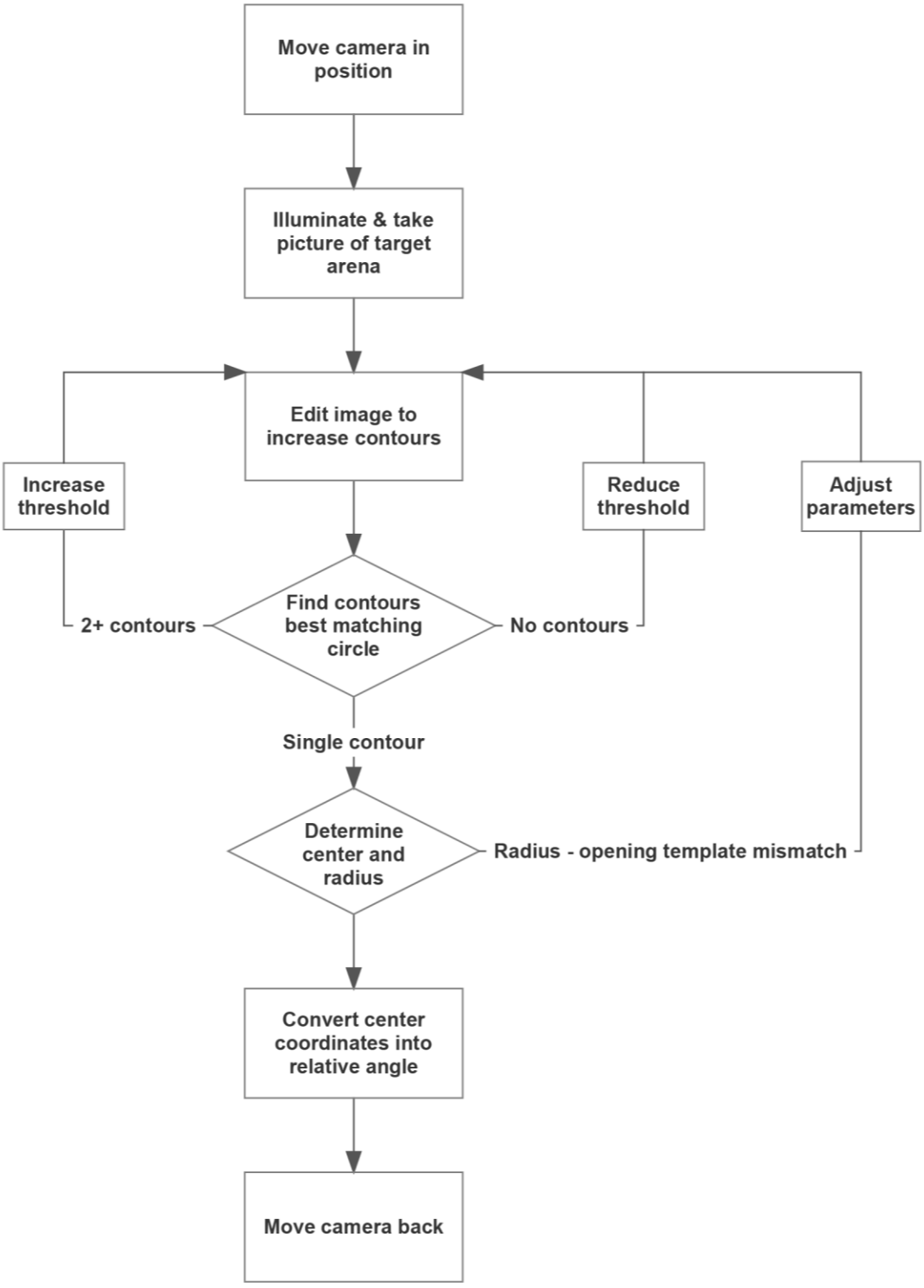

Supplementary Figure 3. Flow chart of algorithm used in determining position of arena-lid opening.

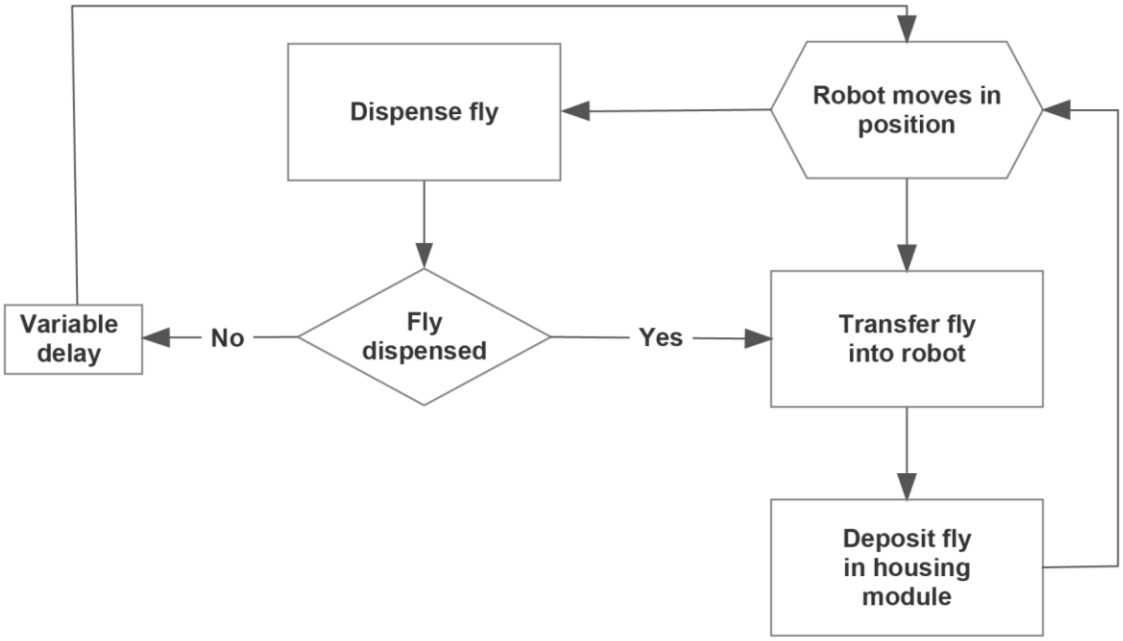

Supplementary Figure 4. Flow chart of sub-routine employed to achieve automated virgining. Preparatory manual steps are omitted. Close-circuit experimentation is possible once flies are deposited in housing module. Note that *variable delay* denotes interval between virgining attempts.

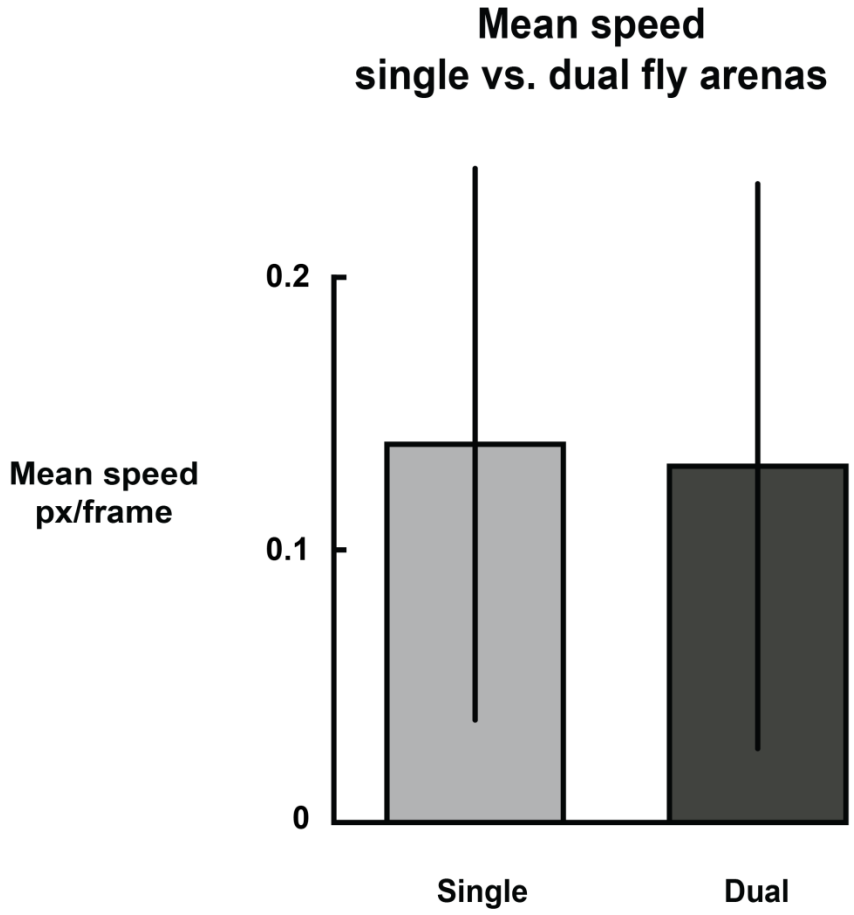

Supplementary Figure 5. Mean speed of flies with a neighboring fly (separated by clear porous fence) compared to mean speed of flies with an empty neighboring arena-half. Error bars denote 1/- 1 SEM.

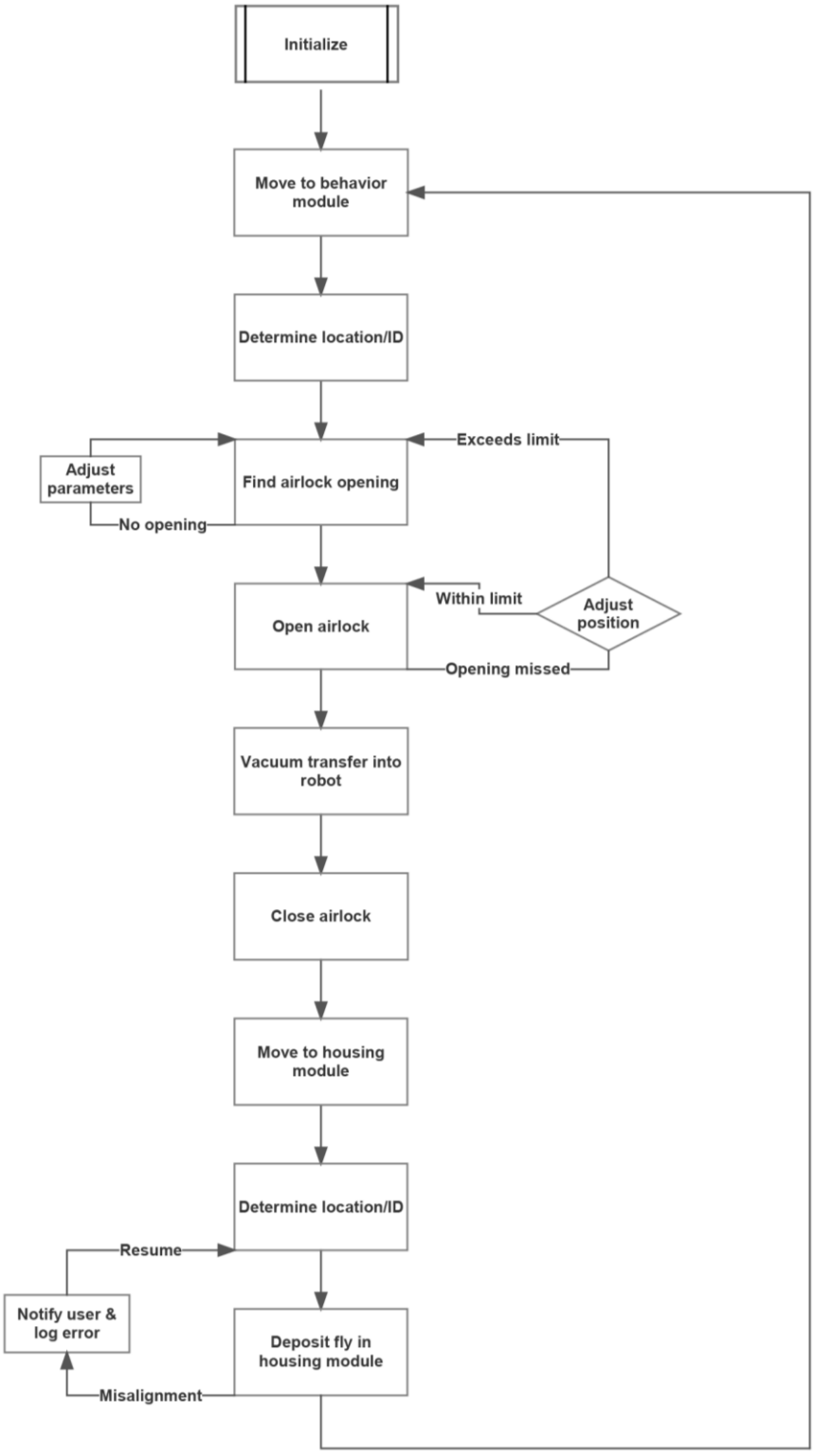

Supplementary Figure 6. Flow chart of routine used to transport a sequence of flies from individual arenas in the behavioral module into individual wells in the housing module.

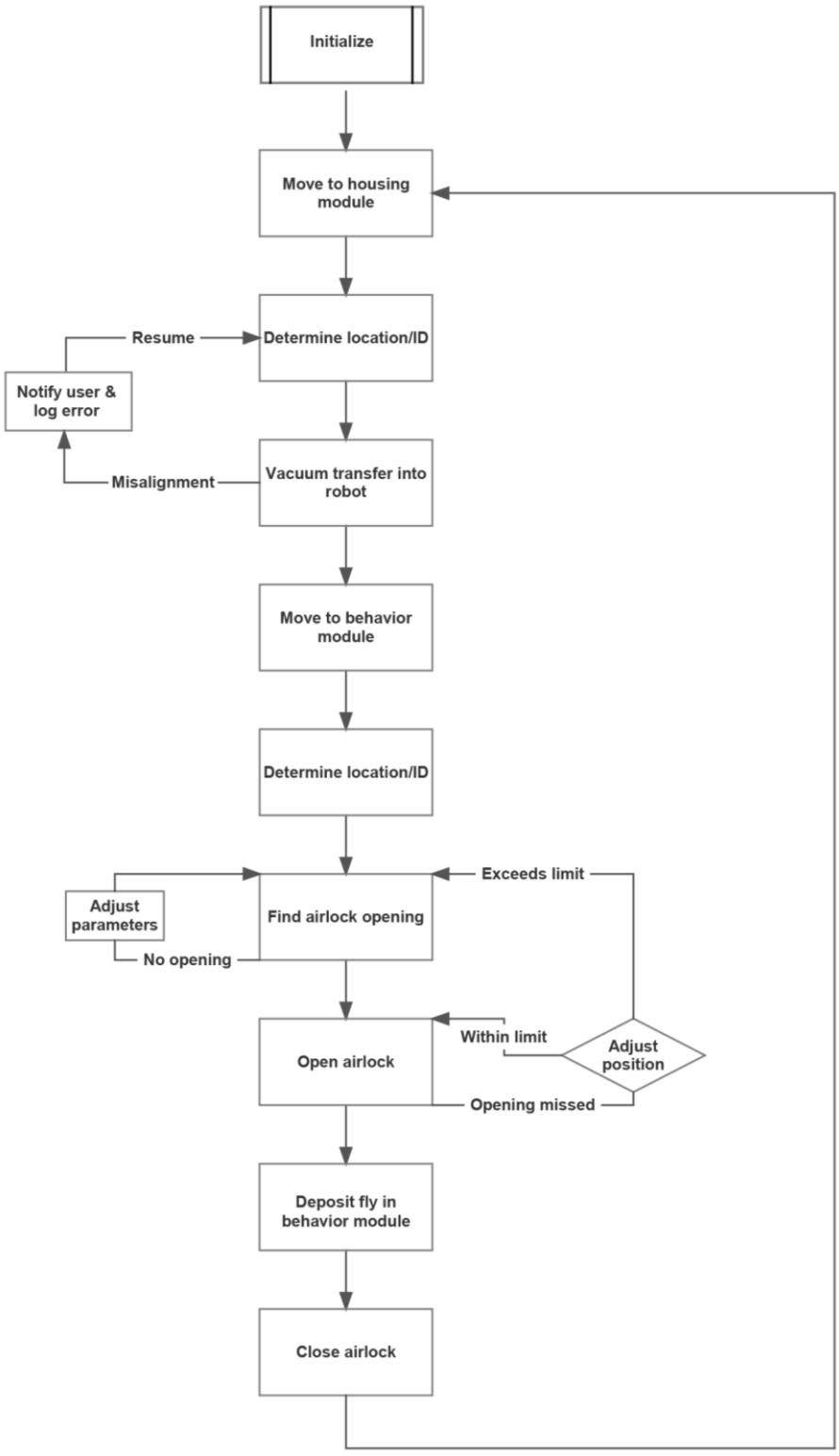

Supplementary Figure 7. Flow chart of routine used to transport a sequence of flies from individual wells in the housing module into individual arenas in the behavioral module.

Supplementary Video 1.

https://www.dropbox.com/sh/8qtvbjux34frebn/AABsovDJv6nvM9UL6W3Nx_kSa?dl=0

Time-lapse video of robot handling awake flies. Flies are moved from housing module into behavior module. Video is sped up to 50x real-time. Actual time required to transport flies shown was 18:57. Top: Birds-eye view. Bottom: Side-view. Note that scenes shown at top and bottom do not reflect the same handling instance.

Supplementary Video 2.

https://www.dropbox.com/sh/8qtvbjux34frebn/AABsovDJv6nvM9UL6W3Nx_kSa?dl=0

Animation of manual preparatory steps required and automatic steps performed to allow robot virgining. Bottom: Days from depositing parents into vial. Note that transport of only one fly is depicted. Actual virgining function includes repetition of *deposit* and *transport* steps. See **Supplementary Figure 4** for more information.

Supplementary Table 1. Withdrawal strategies employed by the robot to evacuate arenas. Strategies correspond to colors in **Figure 3** in order of legend**.**

Strategy	**Summary**
Dislodge	Three 50 ms air bursts followed by continuous vacuum
Rotate	Continuous vacuum while moving along the arena edge
Patience	Continuous vacuum for 3 seconds
Force	One 500 ms air burst followed by continuous vacuum

References

Abreu, M. S., Giacomini, A. C. V. V., Kalueff, A. V., & Barcellos, L. J. G. (2016). The smell of "anxiety": Behavioral modulation by experimental anosmia in zebrafish. *Physiology & Behavior*, *157*, 67–71. http://doi.org/10.1016/j.physbeh.2016.01.030

Albrecht, D. R., & Bargmann, C. I. (2011). High-content behavioral analysis of Caenorhabditis elegans in precise spatiotemporal chemical environments. *Nature Methods*, *8*(7), 599–605. http://doi.org/10.1038/nmeth.1630

Alem, S., Perry, C. J., Zhu, X., Loukola, O. J., Ingraham, T., Søvik, E., & Chittka, L. (2016). Associative Mechanisms Allow for Social Learning and Cultural Transmission of String Pulling in an Insect. *PLOS Biology*, *14*(10), e1002564. http://doi.org/10.1371/journal.pbio.1002564

Bartholomew, N. R., Burdett, J. M., VandenBrooks, J. M., Quinlan, M. C., Call, G. B., Nilson, T. L., … Chambers, R. P. (2015). Impaired climbing and flight behaviour in Drosophila melanogaster following carbon dioxide anaesthesia. *Scientific Reports*, *5*, 15298. http://doi.org/10.1038/srep15298

Billeter, J.-C., & Levine, J. D. (2015). The role of cVA and the Odorant binding protein Lush in social and sexual behavior in Drosophila melanogaster. *Frontiers in Ecology and Evolution*, *3*. http://doi.org/10.3389/fevo.2015.00075

Bloch Qazi, M. C., Heifetz, Y., & Wolfner, M. F. (2003). The developments between gametogenesis and fertilization: Ovulation and female sperm storage in Drosophila melanogaster. *Developmental Biology*, *256*(2), 195–211. http://doi.org/10.1016/S0012-1606(02)00125-2

Branson, K., Robie, A. A., Bender, J., Perona, P., & Dickinson, M. H. (2009). High-throughput ethomics in large groups of Drosophila. *Nature Methods*, *6*(6), 451–457. http://doi.org/10.1038/nmeth.1328

Buchanan, S. M., Kain, J. S., & de Bivort, B. L. (2015). Neuronal control of locomotor handedness in Drosophila. *Proceedings of the National Academy of Sciences*, *112*(21), 6700–6705. http://doi.org/10.1073/pnas.1500804112

Burg, E. D., Langan, S. T., & Nash, H. A. (2013). Drosophila social clustering is disrupted by anesthetics and in narrow abdomen ion channel mutants. *Genes, Brain and Behavior*, *12*(3), 338–347.

http://doi.org/10.1111/gbb.12025

Card, G., & Dickinson, M. H. (2008). Visually Mediated Motor Planning in the Escape Response of Drosophila. *Current Biology*, *18*(17), 1300–1307. http://doi.org/10.1016/j.cub.2008.07.094

Chalasani, S. H., Chronis, N., Tsunozaki, M., Gray, J. M., Ramot, D., Goodman, M. B., & Bargmann, C. I. (2007). Dissecting a circuit for olfactory behaviour in Caenorhabditis elegans. *Nature*, *450*(7166), 63–70. http://doi.org/10.1038/nature06292

Chung, K., Kim, Y., Kanodia, J. S., Gong, E., Shvartsman, S. Y., & Lu, H. (2011). A microfluidic array for large-scale ordering and orientation of embryos. *Nature Methods*, *8*(2), 171–176. http://doi.org/10.1038/nmeth.1548

Colinet, H., & Renault, D. (2012). Metabolic effects of CO2 anaesthesia in Drosophila melanogaster. *Biology Letters*, *8*(6), 1050–1054. http://doi.org/10.1098/rsbl.2012.0601

Colomb, J., Reiter, L., Blaszkiewicz, J., Wessnitzer, J., & Brembs, B. (2012). Open source tracking and analysis of adult Drosophila locomotion in Buridan's paradigm with and without visual targets. *PLoS ONE*, *7*(8), 1–12. http://doi.org/10.1371/journal.pone.0042247

Contractor, N. S., & DeChurch, L. A. (2014). Integrating social networks and human social motives to achieve social influence at scale. *Proceedings of the National Academy of Sciences*, *111*(Supplement_4), 13650–13657. http://doi.org/10.1073/pnas.1401211111

Crane, M. M., Stirman, J. N., Ou, C.-Y., Kurshan, P. T., Rehg, J. M., Shen, K., & Lu, H. (2012). Autonomous screening of C. elegans identifies genes implicated in synaptogenesis. *Nature Methods*, *9*(10), 977–80. http://doi.org/10.1038/nmeth.2141

Croy, I., Bojanowski, V., & Hummel, T. (2013). Men without a sense of smell exhibit a strongly reduced number of sexual relationships, women exhibit reduced partnership security – A reanalysis of previously published data. *Biological Psychology*, *92*(2), 292–294. http://doi.org/10.1016/j.biopsycho.2012.11.008

Dall, S. R. X., Houston, A. I., & McNamara, J. M. (2004). The behavioural ecology of personality: consistent individual differences from an adaptive perspective. *Ecology Letters*, *7*(8), 734–739.

http://doi.org/10.1111/j.1461-0248.2004.00618.x

Gargano, J. W., Martin, I., Bhandari, P., & Grotewiel, M. S. (2005). Rapid iterative negative geotaxis (RING): a new method for assessing age-related locomotor decline in Drosophila. *Experimental Gerontology*, *40*(5), 386–395. http://doi.org/10.1016/j.exger.2005.02.005

Giacomotto, J., & Ségalat, L. (2010). High-throughput screening and small animal models, where are we? *British Journal of Pharmacology*, *160*(2), 204–216. http://doi.org/10.1111/j.1476-5381.2010.00725.x

Gibson, W. T., Gonzalez, C. R., Fernandez, C., Ramasamy, L., Tabachnik, T., Du, R. R., … Anderson, D. J. (2015). Behavioral Responses to a Repetitive Visual Threat Stimulus Express a Persistent State of Defensive Arousal in Drosophila. *Current Biology*, *25*(11), 1401–1415. http://doi.org/10.1016/j.cub.2015.03.058

Honegger, Kyle; Smith, Matthew; Turner, Glenn; de Bivort, B. (2016). Animal-to-Animal Variation in Odor Preference and Neural Representation of Odors. *APS March Meeting 2016*. http://doi.org/2016APS..MARK35008H

Kacsoh, B. Z., Bozler, J., Ramaswami, M., & Bosco, G. (2015). Social communication of predator-induced changes in Drosophila behavior and germ line physiology. *eLife*, *4*. http://doi.org/10.7554/eLife.07423

Kain, J. S., Stokes, C., & de Bivort, B. L. (2012). Phototactic personality in fruit flies and its suppression by serotonin and white. *Proceedings of the National Academy of Sciences*, *109*(48), 19834–19839. http://doi.org/10.1073/pnas.1211988109

Kain, J. S., Zhang, S., Akhund-Zade, J., Samuel, A. D. T., Klein, M., & de Bivort, B. L. (2015). Variability in thermal and phototactic preferences in Drosophila may reflect an adaptive bet-hedging strategy. *Evolution*, *69*(12), 3171–3185. http://doi.org/10.1111/evo.12813

Kaur, K., Simon, A. F., Chauhan, V., & Chauhan, A. (2015). Effect of bisphenol A on Drosophila melanogaster behavior – A new model for the studies on neurodevelopmental disorders. *Behavioural Brain Research*, *284*, 77–84. http://doi.org/10.1016/j.bbr.2015.02.001

Kossinets, G. (2006). Empirical Analysis of an Evolving Social Network. *Science*, *311*(5757), 88–90. http://doi.org/10.1126/science.1116869

Kumar, S. S., Sun, Y., Zou, S., & Hong, J. (2016). 3D Holographic Observatory for Long-term Monitoring of Complex Behaviors in Drosophila. *Scientific Reports*, *6*(1), 33001. http://doi.org/10.1038/srep33001

Larsson, M. C., Domingos, A. I., Jones, W. D., Chiappe, M. E., Amrein, H., & Vosshall, L. B. (2004). Or83b Encodes a Broadly Expressed Odorant Receptor Essential for Drosophila Olfaction. *Neuron*, *43*(5), 703–714. http://doi.org/10.1016/j.neuron.2004.08.019

McKay, R. R., Chen, D.-M., Miller, K., Kim, S., Stark, W. S., & Shortridge, R. D. (1995). Phospholipase C Rescues Visual Defect in norpA Mutant of Drosophila melanogaster. *Journal of Biological Chemistry*, *270*(22), 13271–13276. http://doi.org/10.1074/jbc.270.22.13271

Medici, V., Vonesch, S. C., Fry, S. N., & Hafen, E. (2015). The FlyCatwalk: A High-Throughput Feature-Based Sorting System for Artificial Selection in Drosophila. *G3: Genes, Genomes, Genetics*, *5*(3), 317–327. http://doi.org/10.1534/g3.114.013664

Nilsen, S. P., Chan, Y.-B., Huber, R., & Kravitz, E. A. (2004). Gender-selective patterns of aggressive behavior in Drosophila melanogaster. *Pnas*, *101*(33), 12342–12347. http://doi.org/10.1073/pnas.0404693101

Pandey, U. B., & Nichols, C. D. (2011). Human Disease Models in Drosophila melanogaster and the Role of the Fly in Therapeutic Drug Discovery. *Drug Delivery*, *63*(2), 411–436. http://doi.org/10.1124/pr.110.003293.411

Pasquaretta, C., Battesti, M., Klenschi, E., Bousquet, C. A. H., Sueur, C., & Mery, F. (2016). How social network structure affects decision-making in Drosophila melanogaster. *Proceedings of the Royal Society of London B: Biological Sciences*, *283*(1826). Retrieved from http://rspb.royalsocietypublishing.org/content/283/1826/20152954

Perron, J. M., Huot, L., Corrivault, G.-W., & Chawla, S. S. (1972). Effects of carbon dioxide anaesthesia on Drosophila melanogaster. *Journal of Insect Physiology*, *18*(10), 1869–1874.

http://doi.org/10.1016/0022-1910(72)90157-6

Pfeiffenberger, C., Lear, B. C., Keegan, K. P., & Allada, R. (2010). Locomotor Activity Level Monitoring Using the Drosophila Activity Monitoring (DAM) System. *Cold Spring Harbor Protocols*, *2010*(11), pdb.prot5518-prot5518. http://doi.org/10.1101/pdb.prot5518

Pike, T. W., Samanta, M., Lindstrom, J., & Royle, N. J. (2008). Behavioural phenotype affects social interactions in an animal network. *Proceedings of the Royal Society B: Biological Sciences*, *275*(1650), 2515–2520. http://doi.org/10.1098/rspb.2008.0744

Ramdya, P., Lichocki, P., Cruchet, S., Frisch, L., Tse, W., Floreano, D., & Benton, R. (2014). Mechanosensory interactions drive collective behaviour in Drosophila. *Nature*, *519*(7542), 233–236. http://doi.org/10.1038/nature14024

Ronderos, D. S., & Smith, D. P. (2010). Activation of the T1 Neuronal Circuit is Necessary and Sufficient to Induce Sexually Dimorphic Mating Behavior in Drosophila melanogaster. *Journal of Neuroscience*, *30*(7), 2595–2599. http://doi.org/10.3389/fevo.2015.00075

Saleem, S., Ruggles, P. H., Abbott, W. K., & Carney, G. E. (2014). Sexual experience enhances Drosophila melanogaster male mating behavior and success. *PLoS ONE*, *9*(5). http://doi.org/10.1371/journal.pone.0096639

Savall, J., Ho, E. T. W., Huang, C., Maxey, J. R., & Schnitzer, M. J. (2015). Dexterous robotic manipulation of alert adult Drosophila for high-content experimentation. *Nature Methods*, *12*(7), 657–60. http://doi.org/10.1038/nmeth.3410

Schneider, J., Dickinson, M. H., & Levine, J. D. (2012). Social structures depend on innate determinants and chemosensory processing in Drosophila. *Proceedings of the National Academy of Sciences of the United States of America*, (Suppl 2), 17174–9. http://doi.org/10.1073/pnas.1121252109

Schuett, W., Dall, S. R. X., Baeumer, J., Kloesener, M. H., Nakagawa, S., Beinlich, F., & Eggers, T. (2011). Personality variation in a clonal insect: The pea aphid, Acyrthosiphon pisum. *Developmental Psychobiology*, *53*(6), 631–640. http://doi.org/10.1002/dev.20538

Simon, A. F., Chou, M. T., Salazar, E. D., Nicholson, T., Saini, N., Metchev, S., & Krantz, D. E. (2012).

A simple assay to study social behavior in Drosophila: Measurement of social space within a group. *Genes, Brain and Behavior*, *11*(2), 243–252. http://doi.org/10.1111/j.1601-183X.2011.00740.x

Trannoy, S., Chowdhury, B., & Kravitz, E. A. (2015). Handling alters aggression and " loser " effect formation in Drosophila melanogaster. *Learning & Memory*, *22*, 64–68. http://doi.org/10.1101/lm.036418.114

Turner, R. M., Derryberry, S. L., Kumar, B. N., Brittain, T., Zwiebel, L. J., Newcomb, R. D., & Christie, D. L. (2014). Mutational analysis of cysteine residues of the insect odorant co-receptor (Orco) from drosophila melanogaster reveals differential effects on agonist- and odorant-tuning receptor-dependent activation. *Journal of Biological Chemistry*, *289*(46), 31837–31845. http://doi.org/10.1074/jbc.M114.603993

Whitworth, A. J., Wes, P. D., & Pallanck, L. J. (2006). Drosophila models pioneer a new approach to drug discovery for Parkinson's disease. *Drug Discovery Today*, *11*(3–4), 119–126. http://doi.org/10.1016/S1359-6446(05)03693-7

Yang, Z., Bertolucci, F., Wolf, R., & Heisenberg, M. (2013). Flies cope with uncontrollable stress by learned helplessness. *Current Biology*, *23*(9), 799–803. http://doi.org/10.1016/j.cub.2013.03.054